Meteoritics & Planetary Science 33, 1317–1333 (1998)

Petrography and geochemistry of target rocks and impactites from the Ilyinets Crater, Ukraine

EUGENE P. GUROV[1], CHRISTIAN KOEBERL[2]* AND WOLF UWE REIMOLD[3]

[1]Institute of Geological Sciences, Ukrainian Academy of Sciences, 55b Chkalov Street, Kiev 252601, Ukraine
[2]Institute of Geochemistry, University of Vienna, Althanstrasse 14, A-1090 Vienna, Austria
[3]Department of Geology, University of the Witwatersrand, Johannesburg 2050, South Africa
*Correspondence author's e-mail address: christian.koeberl@univie.ac.at

(Received 1998 March 27; accepted in revised form 1998 September 3)

Abstract–The ~400 Ma old Ilyinets impact structure was formed in the Precambrian basement of the Ukrainian Shield and is now mostly covered by Quaternary sediments. Various impact breccias and melts are exposed in its southern section. The crater is a complex structure with a central uplift that is surrounded by an annular deposit of breccias and melt rocks. In the annulus, brecciated basement rocks are overlain by up to 80 m of glass-poor suevitic breccia, which is overlain (and partly intercalated) by glass-rich suevite with a thickness of up to 130 m. Impact-melt rocks occur within and on top of the suevites—in some cases in the form of devitrified bomb-shaped impact-glass fragments. We have studied the petrographic and geochemical characteristics of 31, mostly shocked, target rock samples (granites, gneisses, and one amphibolite) obtained from drill cores within the structure, and impact breccias and melt rock samples from drill cores and surface exposures. Multiple sets of planar deformation features (PDFs) are common in quartz, potassium feldspar, and plagioclase of the shocked target rocks. The breccias comprise more or less devitrified impact melt with shocked clasts. The impact-melt rocks ("bombs") show abundant vesicles and, in some cases, glass is still present as brownish patches and schlieren. All impact breccias (including the melt rocks) are strongly altered and have significantly elevated K contents and lower Na contents than the target rocks. The alteration could have occurred in an impact-induced hydrothermal system. The bomb-shaped melt rocks have lower Mg and Ca contents than other rock types at the crater. Compared to target rocks, only minor enrichments of siderophile element contents (*e.g.*, Ni, Co, Ir) in impact-melt rocks were found.

INTRODUCTION

The Ilyinets impact structure is one of seven confirmed impact structures in the Ukraine (Fig. 1). It is situated in the western part of the Ukrainian Shield and is centered at 49°07' N and 29°06' E, 45 km southeast of the town of Vinnitsa, within the basin formed between the Sobik and the Sob rivers. The first description of rocks with an unusual texture was made in 1861 by K. I. Pheophylaktov (cf., Masaitis *et al.*, 1980). The Ilyinets structure was commonly interpreted to be of volcanic origin, until Masaitis (1973) and Valter and Ryabenko (1973) demonstrated its meteorite impact origin. Subsequently, various aspects of the Ilyinets impact structure have been described in several papers in the Russian literature (*e.g.*, Valter, 1975; Valter and Ryabenko, 1977; Masaitis *et al.*, 1980; Gurov and Ryabenko, 1984; Gurov and Gurova, 1991b).

FIG. 1. Schematic map of the Ukraine, with seven known impact structures (bold; filled circles). Major cities are also shown. The hatched area indicates the extent of the Ukrainian shield.

The Ilyinets structure is a deeply eroded complex crater ~3 to 4 km in diameter. The crater basement is composed of crystalline rocks of the Ukrainian Shield (Fig. 2). Biotite granites are the predominant target rocks, whereas gneisses, amphibolites, and schists are less voluminous and occur mainly in the northern part of the crater. Fragments of argillites and sandstones occur in suevites but have never been observed *in situ* on the surface of crystalline basement (Gurov and Gurova, 1991b). The crater is currently buried under some tens of meters of Cenozoic sediments. The structure of the crater was studied using several bore holes drilled mainly in the 1970s. A variety of impact breccias and basement rocks are also exposed in quarries dating to the third and fourth century A.D. and in natural outcrops in the Sobik river valley in the southern part of the crater.

The purpose of the present paper is to summarize the geological and petrological work that has been performed over two decades in the former Soviet Union and that was published only in Russian, and to provide detailed petrographical observations and geochemical data for target rocks and impactites from drill cores 2100, 5006, 5008, 18480, and samples from exposures in the Sobik river valley (Fig. 2). Preliminary results were reported in abstract form by Koeberl *et al.* (1996).

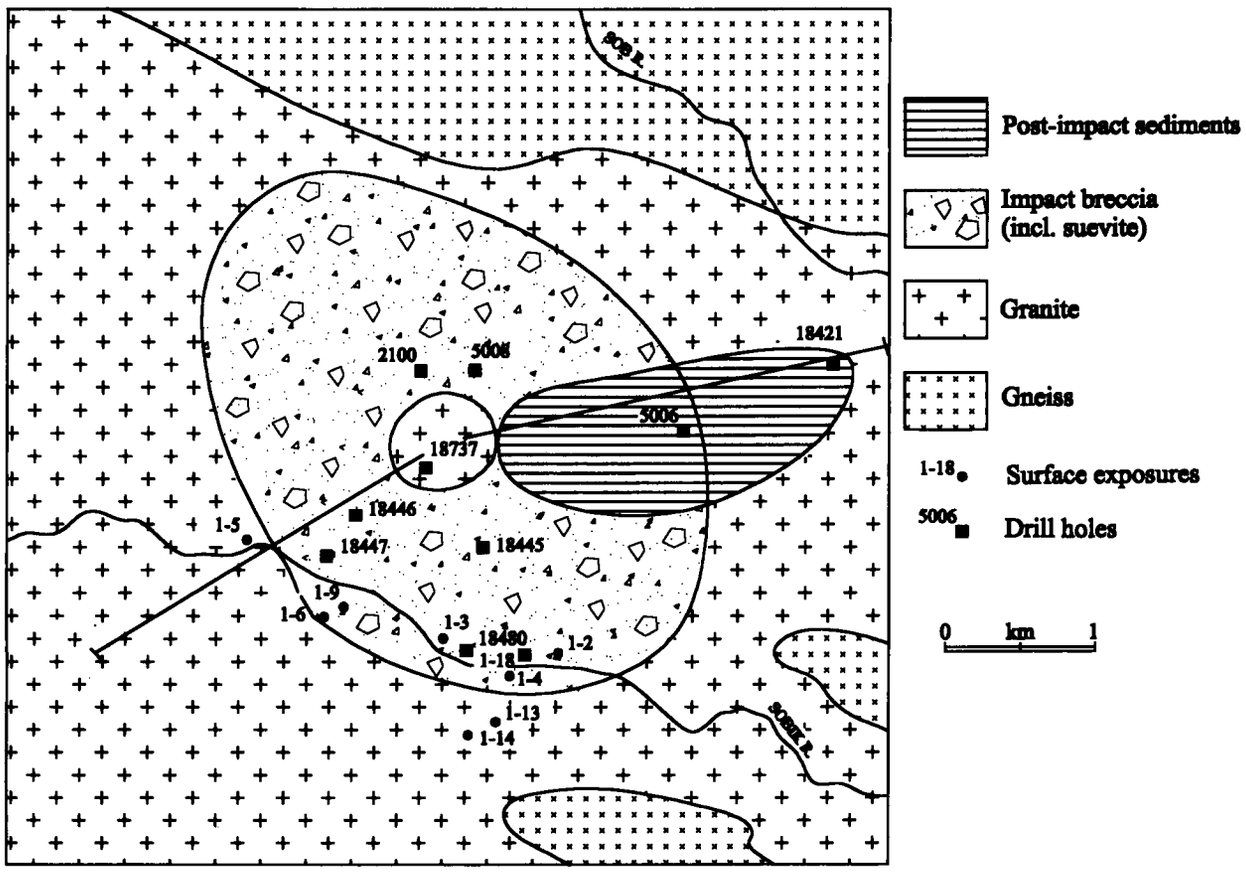

FIG. 2. Schematic map of the Ilyinets impact structure (partly after Gurov and Gurova, 1991b; Masaitis *et al.*, 1980; and Valter and Ryabenko, 1977). The Cenozoic rocks that cover the area have been omitted for clarity. The locations of the quarries and surface exposures (circles), as well as the locations of the drill cores (squares: four- and five-digit numbers), are indicated. Inner circle shows central uplift. The rivers Sob and Sobik are also indicated.

GENERAL GEOLOGY OF THE ILYINETS IMPACT STRUCTURE

The information in this section is mostly a summary of data from Masaitis *et al.* (1980), Valter and Ryabenko (1977), Gurov and Gurova (1991b), and some new observations from our drill core samples. The Ilyinets structure is a slightly oblong structure (dimensions ~4.1 × 3.4 km) with the major axis from the northwest to the southeast (Fig. 2). The crater floor drops gently from the outer limits of the structure to the base of the central uplift. Compared to the surrounding stratigraphic location of the strata, the depth of the circular depression is 270–300 m, as shown by data from drill holes 5008 and 2100, which are located ~0.6–0.8 km to the north and northeast from the crater center, in the deepest part of the annular structure.

The crater floor is formed by autochthonous monomict granitic breccias, with a gradual transition from monomict breccias to fractured crystalline basement. The thickness of these autochthonous breccias varies from 50 m in the outer part to 70 m around the base of the central uplift. Exposures occur in the valley of the Sobik river at a distance of 200 to 400 m from the outer limit of the crater structure. Drill core studies show that the crater floor, as defined by the top of the autochthonous breccias, is irregular. The transition of these rocks to polymictic suevites is gradual over a zone several tens of meters thick, in which the block size gradually decreases upwards.

The crater is filled with suevitic breccias. Suevites with low-glass content form the lower layer in the crater, with a thickness ranging from ~100 m around the central peak to ~30–50 m in the outer part of the structure. The size of mineral and rock fragments in the polymict breccia ranges mostly from a few millimeters to 8 cm and very rarely up to several tens of centimeters. The lower part of the suevite layer contains predominantly crystalline rock clasts, with biotite granite as the main component. The glass content increases from <1 vol% in the lower part of the glass-poor suevite breccia to 5–10 vol% in its upper part, directly underlying the glass-rich suevite zone. Rare fragments of argillites and siltstones occur in the upper part of the allochthonous breccia section.

Glass-rich suevites form the upper horizon of the allochthonous crater fill of the Ilyinets structure. In the Russian literature, it is customary to designate an impact rock as a suevite only if the glass content is 10 vol%, which may lead to some confusion when referring to Russian publications. In keeping with the standard international nomenclature (*e.g.*, Stöffler and Grieve, 1994), we use the term "suevite" for any glass-bearing polymict impact breccia. At the top of the suevite layer, the content of glass fragments and particles increases to 30–40 vol%. The glass-rich suevite forms an annular layer around the central peak. The thickness of this layer ranges from ~80–130 m in the inner part of the crater, to close to zero in the outer part, at a distance of ~1.3–1.7 km from the crater center. Crystalline rock clasts in suevites are predominantly derived from granite and gneiss; but in the upper part of this suevite section, fragments of sedimentary rocks (of unknown age) are abundant. Numerous fragments and boulders of argillites occur in suevites

exposed in the quarries in the Sobik river valley. The size of the biggest blocks of sedimentary rocks reaches up to 1.5 m in diameter. The abundance of argillite and siltstone fragments in suevites intersected in hole 5008 is ~8 vol% at a depth of 20 m and decreases to 3–4 vol% at a depth of 50 m. The last argillite fragment was found at 120 m depth. Fragments of sedimentary rocks occur to ~55 m depth in the drill hole 5006 in the outer parts of the crater.

Glass "bombs," similar to those described from the Ries crater in Germany (cf., Stähle, 1972), occur in the uppermost horizon of suevites exposed in quarries in the southern part of the crater. In this zone, the horizon with glass bombs overlies a sheet of impact-melt rock. In some cases, glass bombs are preserved in the melt zone near the contact with the suevites. Bombs occur in the form of drops, ropes, cakes ("flädle"), and irregular shapes. The preserved thickness of this fallback suevite horizon is up to 10 m, but its partial erosion on the slopes of the Sobik river valley may have reduced the original thickness.

Impact-melt rocks form a layer in the southern area of the Ilyinets crater. Also, dikelike melt bodies in breccias occur to the north of the central peak. The impact-melt layer is exposed at the present-day surface in quarries and natural exposures in the Sobik river valley. In outcrops, the impact-melt body dips subhorizonatally in a northerly direction underneath the suevite but was intersected by drill holes over an area of ~1.5 km^2. The thickness of the melt body is ~30 m, as determined in drill holes 18480 and 18445, which penetrate through the melt layer into underlying suevites. The uppermost horizon of the melt layer (~1 m thick) contains numerous inclusions of crystalline rocks, with sizes ranging from a few millimeters to ~1 m. Inclusions of glass bombs occur in the upper 30 cm of the melt zone. The relative abundance of the various rock fragments in the melt rock was obtained by counting fragments in two quarries on the slopes of the Sobik river valley and is given in Table 1. The main inclusion type in the melt rock is granite, with relative abundances of the rock fragments in the melt rock being similar to those of crystalline rocks in the crater basement (Valter and Ryabenko, 1977).

Voids with average diameters of 10 to 15 cm occur in the upper part of the melt section. Most are filled with brown clay, but rare agate nodules were found as well. They are generally small, but one large and well-developed agate nodule with a size of 32 × 25 × 14.5 cm was found in the melt. A section of this nodule (in contact with impact melt) is shown in Fig. 3a. Agates, which are hydrothermal vesicle fillings that probably formed in a low-temperature postimpact hydrothermal system at the structure, have been found recently in Finnish impact structures by Kinnunen and Lindqvist (1998). These authors suggested that there are few differences between agates related to volcanic rocks and those related to impactites. Figure 3b shows the microstructure of Ilyinets agate in contact with altered impact-melt rock. No extensive recrystallization, microbanding, or chicken-wire structure (Kinnunen and Lindqvist, 1998) was found in our specimens.

TABLE 1. Abundance of clast types in impact melt breccia from surface exposures at the Ilyinets structure.

Location	Granite	Gneiss	Amphibolite	Sediment	Number of clasts
I-2	93.3	8.7	–	–	11
I-6	89.4	7.1	2.1	1.4	178

The clasts in I-2 range in size from 5 to 25 cm and were found in an area of 3.3 m^2; the clasts in I-6 range in size from 1 to 20 cm and an area of 9.9 m^2 was counted. For location of quarries, see Fig. 2.

In contrast to the southern part of the crater, where impact-melt rock occurs as a coherent body, melt rocks occur only as irregular bodies within suevite in the northern part of the structure. Their thickness ranges from a few centimeters to 11 m. Impact-melt rock was intersected in drill hole 2100 in the intervals 34–45 m, 91–93.5 m, 142.5–151.5 m, and 211–213 m. The contacts of the impact-melt rock bodies with the surrounding suevites is steeply dipping at ~60°. These bodies of impact-melt rock were not penetrated in neighboring drill holes.

Relics of postcratering, lacustrine sediments are preserved in the eastern part of the crater, extending from the central uplift to the eastern crater edge and further—to a distance of ~3 km. The thickness of these sediments is 30–40 m. The basal layer is gravel sandstone with numerous fragments of suevites and shock metamorphosed crystalline rocks. Clay, siltstone, and argillite are the main components of postcratering sediments. Palynological investigations by E. M. Andreeva and L. A. Sergeeva (cited in Bistrevskaya *et al.*, 1974; Masaitis *et al.*, 1980; Valter and Ryabenko, 1977) indicate that the sediments are probably of early Devonian age.

Drill core data were used to generate most of the information given above. Figure 4 shows stratigraphic columns of the drill cores discussed here and sampled for the present study. This information was used to construct a schematic cross-section of the structure, as shown in Fig. 5.

SAMPLES AND EXPERIMENTAL METHODS

Four drill cores were investigated (2100, 5006, 5008, and 18480). The stratigraphic columns, from our own observations, are presented in Fig. 4. In core 2100, the total thickness of impact-melt rocks and breccias is 46 m; the deepest impact-melt rock body was encountered between 266 and 282 m. Fragmental breccia occurs to the bottom of the hole at 338 m. Large fragments within the breccia are granites (at 305–310 m and 336–337 m) and gneiss (at 282–292 m and 319–325 m). Very rare glassy fragments were found at 336 m. In core 18480, impact-melt rocks and glass-rich suevites occur between 7 and 38.5 m. Glass-poor suevites extend to 95 m, and fragmental breccia was encountered from 95 to 173 m. In this interval, the most abundant clasts are fresh granites, with some rare gneiss. Only ~1 mm thick calcite veins are present in the rocks. Weakly fractured basement rocks (granite, gneiss, and amphibolite) occur to the bottom of the hole at 253 m. Most of the cores have not been preserved, and only limited core samples are available at the Institute of Geology, Ukrainian Academy of Sciences, Kiev, Ukraine.

For our studies, we cut centimeter- to decimeter-sized sections of the drill cores and surface exposure samples. Thirty-one bulk rock samples were selected for petrographic and chemical analysis. Samples were taken from three of the drill cores at various depths and from six outcrops, with locations listed in Table 2 and shown in Fig. 2. Sample selection was made to obtain a representative selection of the most important (common) target rock and impactite types that had been recognized in macroscopic studies of the cores.

Polished thin sections were prepared from representative matrix areas and impact-melt rocks, as well as from distinctive clasts and target rocks. Optical microscopic studies were carried out using a polarizing microscope, and shock petrographic studies (crystallographic orientations of planar deformation features, PDFs) were made using a four-axis universal stage (in Johannesburg) and a five-axis universal stage (in Kiev), using methods described by Reinhard (1931), Emmons (1943), and Sobolev (1954). Precision of the PDF

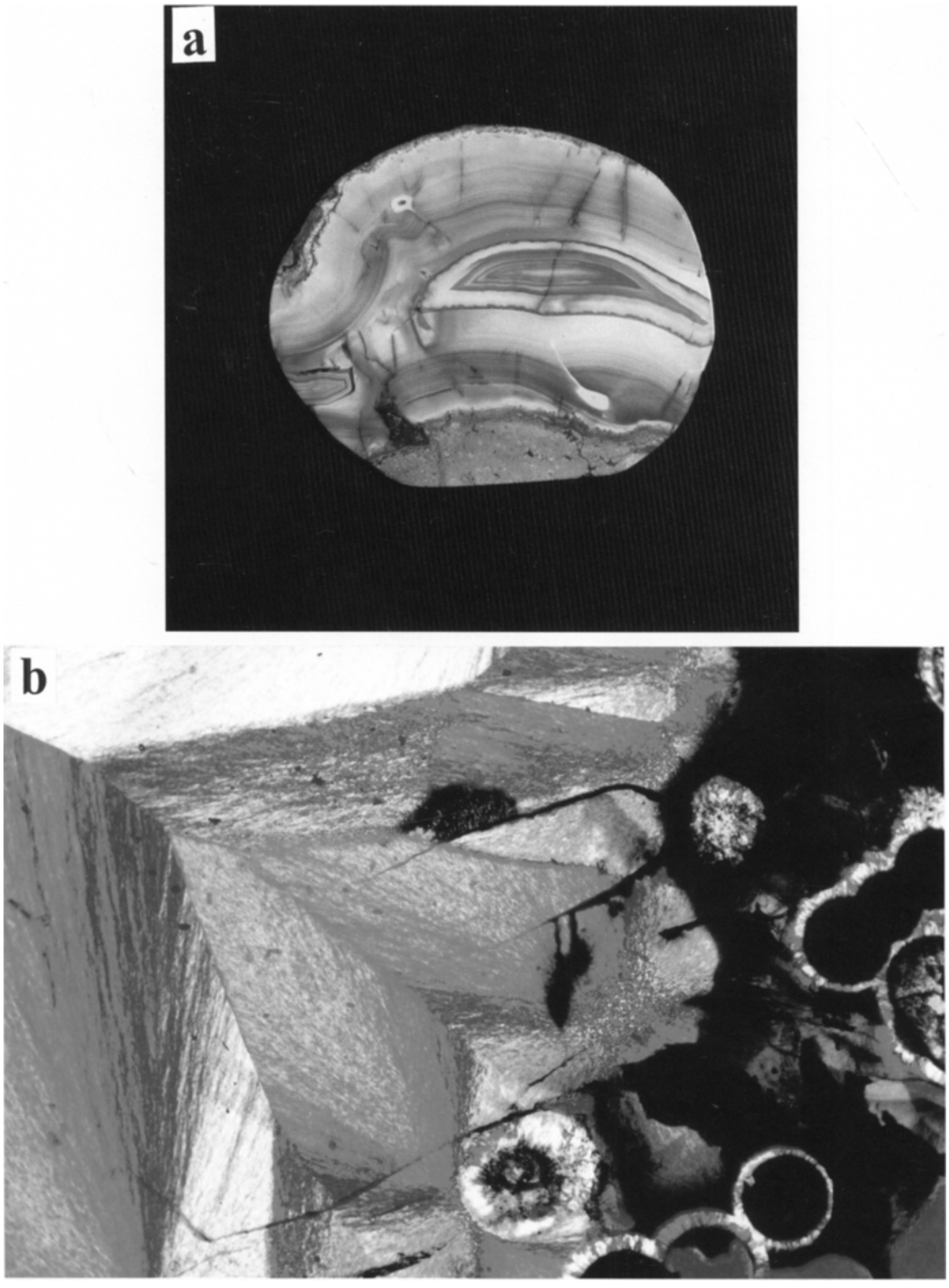

FIG. 3. (a) Polished cross section of agate nodule within impact-melt rock (see contact to melt rock on bottom part) from outcrop I-2 at the Ilyinets impact structure. Long dimension of nodule 16 cm. (b) Microphotograph of agate from I-2 showing contact between altered (partly chloritzed) impact-melt rock (dark area on right side of image) and largely unrecrystallized chalcedony fibers (long dimension of image: 2.5 mm, crossed polars, gypsum plate).

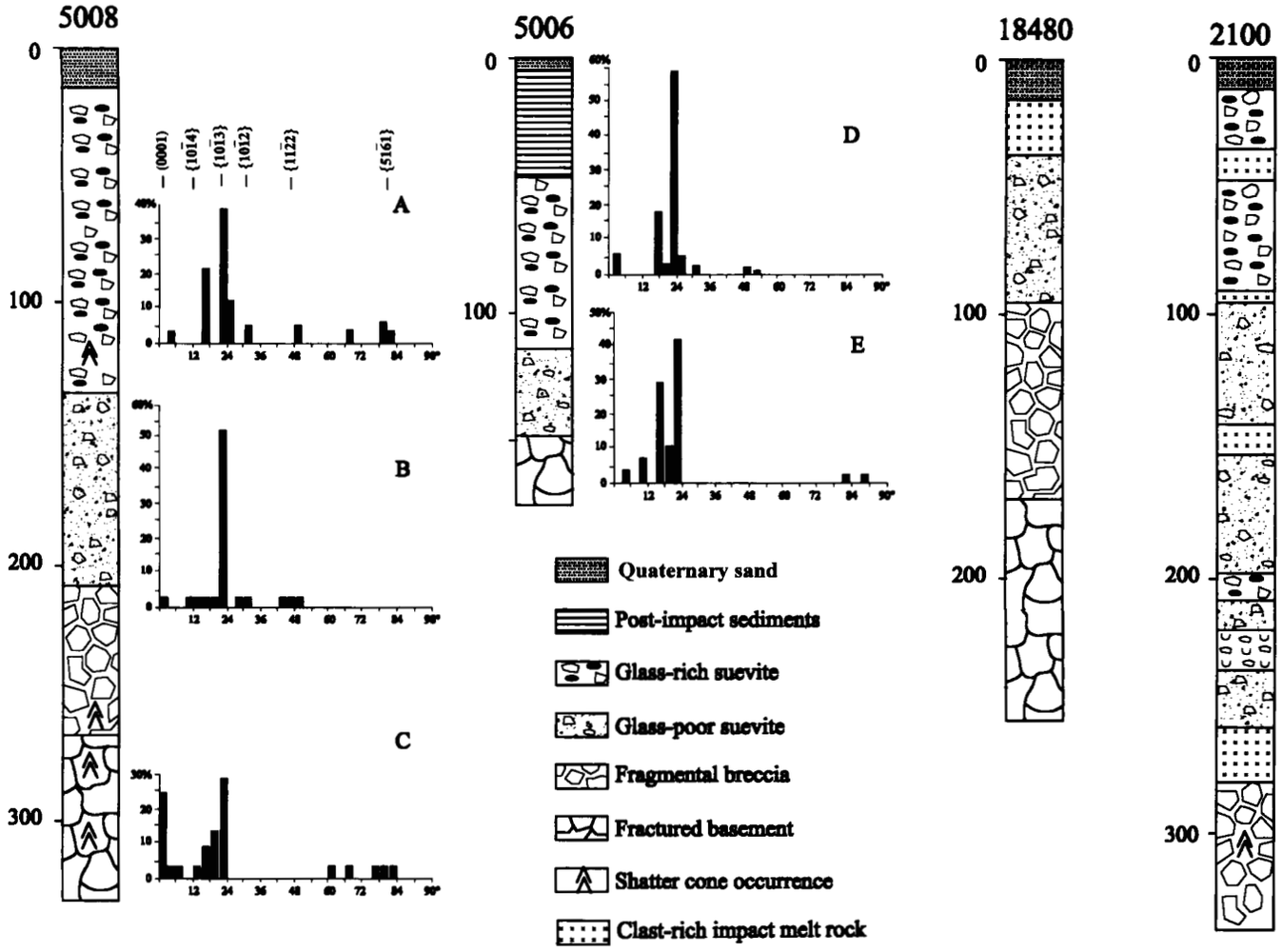

FIG. 4. Stratigraphic column of drill cores 5008 (drilled to 332 m) and 5006 (drilled to 176 m), 18480 (drilled to 253 m), and 2100 (drilled to 328 m). Cores 5008 and 2100 were drilled near the northern flank of the central uplift of the structure; whereas core 5006 was drilled at the eastern limit of the crater and core 18480 was drilled near its southern limit. The stratigraphic columns show different thicknesses of postimpact sediments, suevite, lithic (fragmental) breccia, and brecciated basement. Insets show frequencies (in rel%) of crystallographic orientations of poles of PDFs and the *c*-axis of quartz crystals (in degrees) from various stratigraphic intervals (A = 38 sets in 25 grains, samples from 110 and 126 m; B = 30 sets in 19 grains from 181 and 207 m; C = 33 sets in 27 grains from 304 and 311 m; D = 34 sets in 27 grains from 88.5, 99.0, and 115 m; E = 27 sets in 22 grains from 126 and 141 m).

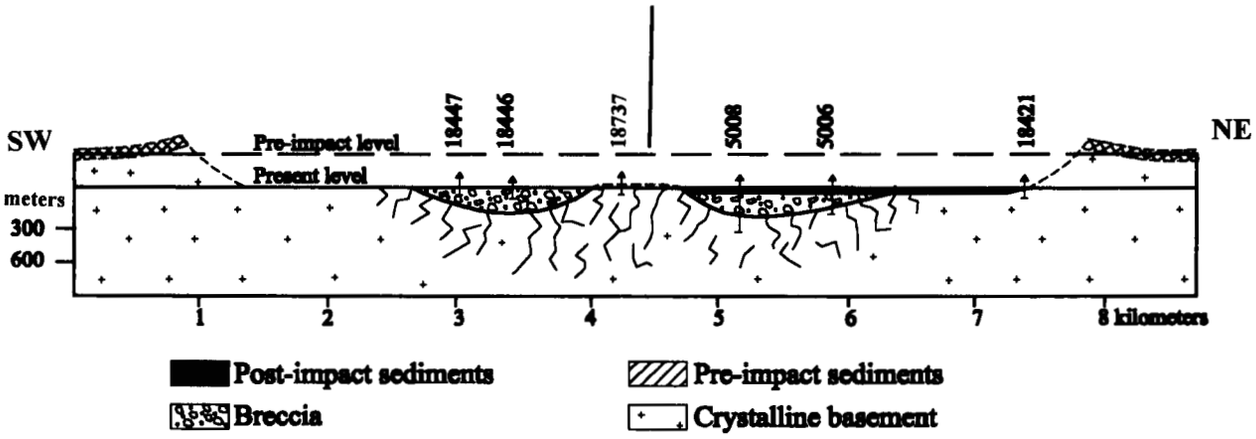

FIG. 5. Schematic southwest to northeast cross-section through the Ilyinets impact structure, as derived from drill core stratigraphy and surface geologic studies. Location of cross-section is indicated in Fig. 2. The inferred position of the preerosion surface is also plotted. The apparent crater floor diameter (after Grieve and Robertson, 1979) was reconstructed using the form and size of the postimpact sedimentary layer. Height and width of the crater rim were reconstructed using data from Gurov and Yamnichenko (1995). No exposures of preimpact sediments remain today in the vicinity of the structure (but were present at the time of the impact, as they are found as rare clasts within breccias).

TABLE 2. Petrographic observations for analyzed samples.

Sample	Location	Petrographic description
I-1	5008-215 m	Large (several centimeters) granite clast in fragmental impact breccia derived from granitic precursor. Granite is strongly shocked (multiple sets of PDFs in quartz and potassium feldspar, potassium feldspar is locally melted; biotite is very intensely kinkbanded; local brecciation zones with strong annealing). Breccia matrix is composed of the same granitic material.
I-2	5008-279 m	Weakly shocked granite fragment. Locally cataclastic breccia zones. Biotite is kinkbanded; a few quartz grains display one set of PDFs, only one grain shows two. Some (minor) annealing. Feldspar is strongly altered; biotite is partially oxidized.
I-3	5008-314 m	Weakly shocked granite fragment. Typical shock fracture pattern, observed in potassium-feldspar; narrow breccia zone is present. Annealing is common. Biotite is kinkbanded; PDFs are seen in only one quartz grain and one plagioclase grain. A few alkali feldspar crystals show mosaicism.
I-4	5008-330 m	Fragmental impact breccia with several, up to 0.5 cm large, granitic clasts; quartz grains contain multiple sets of PDFs. Clasts are moderately to strongly shocked (some rare quartz grains with two sets of PDFs, local melting along brecciation zones). Some strongly tempered feldspar; quartz with apparently curved PDFs that, however, represent individual sets of PDFs in several different crystals. Planar deformation features are often decorated with fluid inclusions but, locally, lamellae are still recognizable.
I-5	18480-160 m	Weakly shocked granite. Narrow annealed zones at grain boundaries (could be preimpact). Few submillimeter brecciation zones (cataclasis). No PDFs, biotite kinkbanding very limited.
I-6	18480-215 m	Weakly shocked, slightly foliated (gneissic) granite. Strong strain deformation, which could be preimpact. Minor cataclasis at interstices and along a few grain boundaries. Less shock deformation than in I-5.
I-7	2100-311 m	Moderately shocked biotite-gneiss (kinkbanding common in biotite, multiple sets of PDFs in quartz).
I-8	18480-178 m	Unshocked, slightly foliated amphibolite (amphibole + plagioclase ± quartz). Contains a few submillimeter, altered shear zones.
I-9	18480-5 m	Strongly altered impact breccia; possibly impact-melt breccia. Contains equally altered, granite-derived clasts, some of which contain quartz grains with remnants of PDFs.
I-10	18480-15 m	Altered, strongly shocked granitoid fragment; devitrified melt with ballen quartz. Patches of light or dark melt. Most quartz clasts are completely annealed. Very similar to strongly shocked (*i.e.*, partially shock melted) samples from Scandinavian impact structures.
I-11	18480-29 m	Fine-grained, devitrified impact-melt breccia, clast-poor (clasts are granite-derived and largely annealed). Some display multiple sets of PDFs in quartz. Many clasts are pure remnants of melted and matrix-incorporated material.
I-12	18480-35 m	As I-11; some quartz clasts have reaction rims with pyroxene and apatite needles.
I-13	18480-38 m	Impact melt breccia; more clast-rich (compared to previous samples). Interesting devitrification textures in wholly melted (but still recognizable) clasts. Matrix is in patches aphanitic. Overall matrix is schlieric. Clasts are generally granite-derived and weakly to strongly shocked. Mafic (biotite-rich) clasts are largely oxidized. Quartz often displays multiple sets of PDFs. Matrix is somewhat vesicular (vesicles are filled with chlorite).
I-14	2100-36 m	Altered, devitrified impact glass with lots of granite-derived clasts. Clasts as in I-13.
I-15	Q.-I-6	Strongly altered, devitrified impact glass; fewer clasts than I-14. This sample may not represent impact-melt breccia but is a largely melted granitoid clast within such breccia.
I-16	Q.-I-9	As sample I-15.
I-17	Q.-I-2	Devitrified impact glass with few clasts. Clasts contain several shocked quartz grains.
I-18	Q.-I-18	Similar to I-17, but less devitrified; also strongly altered. Devitrified impact glass with some rutile needles.
I-19	Q.-I-2	Vesicular, devitrified impact glass with abundant brownish, mafic glass.
I-20	Q.-I-2	As I-19, but more devitrified felsic glass.
I-21	Q.-I-2	Impact-melt breccia of the same type as I-13, with completely melted and devitrified felsic clasts.
I-22	Q.-I-2	Suevite, with devitrified or aphanitic, often schlieric, subangular to angular melt (glass) clasts. Other clasts consist of shale or of granitoid-derived lithic and mineral fragments, besides some carbonate clasts. Vesicles and cracks filled by secondary carbonate. A few quartz clasts have up to two sets of PDFs. A glass fragment with a quartz clast with multiple sets of PDFs was observed. Clastic matrix consists of numerous microclasts but is highly silicified and, thus, it is difficult to discern whether all matrix is clastic or whether there is a melt component.
I-23	Q.-I-2-46A	Strongly shocked, partially melted granitoid fragment; composed of angular crystalline relic grains of quartz and feldspar, many of which are fully annealed and have generally a dull appearance (sintered), set between patches of *in situ* melted, glassy and partially flow-banded patches, believed to represent mainly mafic precursor minerals. Some mineral melts show spherulitic or conchoidal/globular textures.
I-24	Q.-I-2-46B	Clast similar to I-23. Both clasts set into dense and extremely fine-grained (either clastic or aphanitic) matrix with numerous unshocked microclasts (giving a silty appearance). Glassy areas contain a few shocked quartz clasts with PDFs. Samples from location I-2-46 (A+B) are suevite.
I-25	Q.-I-4-12	Moderately shocked biotite-gneiss clast in suevitic breccia with angular glass fragments (resembling shards); some contain strongly shocked (partially melted) clasts. Glass is generally chloritized. Clasts are composed of granitoid material, schist, and biotite-gneiss. Contains some quartz clasts with multiple sets of PDFs and a few that are partially shock melted, as well as several potassium feldspar clasts with one set of PDFs, and one with multiple sets of PDFs. A medium-grained biotite-gneiss clast contains rare quartz grains with multiple sets of PDFs. Many quartz crystals display low-pressure arrays of extension cracks. Kinkbanding in biotite.

TABLE 2. *Continued.*

Sample	Location	Petrographic description
I-26	Q.-I-4-13	Suevite with several large clasts of medium-grained biotite-gneiss. Some locally melted feldspar clasts, quartz fragments with PDFs, diaplectic quartz glass, or melted quartz. Many granitoid clasts have quartz with single or multiple sets (<3) of PDFs. A largely melted plagioclase clast was seen; individual albite twin lamellae are melted. Melt clasts in this sample reach 1 cm in size.
I-27	Q.-I-4-15	Siltstone fragment from within suevite with desiccation cracks.
I-28	Q.-I-6-8	Impact melt breccia; no thin section.
I-29	Q.-I-6-50	Strongly shocked granite fragment (from impact-melt breccia); devitrified glass between strongly annealed relic grains (with thermal alteration textures reminiscent of clasts in Vredefort Granophyre). Relics of mafic precursor minerals are clusters of opaque phases. No shock deformation in relic grains. A few feldspar grains display oxide decoration trails that might mark annealed PDFs.
I-30	Q.-I-9-1	Weakly shocked biotite-granite fragment (no gneissic foliation indicated); some indication of deformation, but no characteristic shock deformation effects. Some biotite is weakly kinkbanded or cracked—especially when wedged between rigid quartz or feldspar grains. Neither shock fracturing nor PDFs were observed. Annealing is limited.
I-31	Q.-I-12	Unshocked, partially annealed granite fragment with little, fine-grained biotite (different lithology from that of sample I-30).

Sample locations contains either quarry (Q.) number or drill core number and depth in meters (see text and Fig. 1).

orientation measurements in Johannesburg were ~3–4°; for the Kiev measurements, they were 1–2°, following methods of Sobolev (1954). X-ray diffractometry was used to study diamonds isolated from impact-melt rocks.

Major element analyses were performed on powdered samples by standard x-ray fluorescence (XRF) procedures (see Reimold *et al.*, 1994, for details on procedures, precision, and accuracy). The concentrations of V, Cu, Y, and Nb were also determined by XRF analysis. All other trace elements were analyzed by instrumental neutron activation analysis (INAA) following procedures described by Koeberl (1993). For most samples, Sr and Zr concentrations were determined by both XRF and INAA; for some of the low abundance samples, Ni data were obtained also by XRF.

RESULTS

Petrography of Samples Analyzed for Chemical Composition

Detailed petrographic studies were made of the 31 samples, representing all different target rock and impactite varieties. A summary of the petrographic findings is provided in Table 2. All samples are either clasts or clasts ± matrix of different types of impact breccias. These include fragmental (lithic), suevitic, and impact-melt breccia (impact-melt rock) (compare Table 2).

A representative selection of target rocks or target rock clasts have been studied. Among these, granitoid clasts are most important, with rare (meta)sedimentary clasts (siltstone, carbonate, and schist). A number of carbonate clasts were observed, for example, in sample I-2. Several types of granitoids were identified, with granitic (biotite-granite) or gneiss (biotite-gneiss) texture. Sample I-8, from the fractured basement in drill-core 18480 (Fig. 4), represents a slightly foliated amphibolitic gneiss.

A detailed discussion of general and previous observations (*e.g.*, Gurov and Gurova, 1991b) regarding shock metamorphism at Ilyinets is given in the next section. Here we only briefly describe information that is pertinent to the newly analyzed samples. Both completely unshocked and shock metamorphosed clasts were observed. Shocked clasts exhibit a wide range of textures—as shown in Fig. 6—ranging from shock fracturing typical of very low (<8 GPa) shock pressures, over single and multiple sets of PDFs in quartz and feldspar (characteristic of the regime between 12 and 30 GPa), and shock mosaicism, to the development of diaplectic quartz glass (30–35 GPa), partial shock melting (35–45 GPa), and bulk shock melting (>45 GPa) (for shock degree classification, see, *e.g.*, Stöffler and Langenhorst, 1994; Grieve *et al.*, 1996; Huffman and Reimold, 1996). Crystallographic orientations of PDFs in quartz from these samples are plotted in Fig. 7 and show shock characteristic angles. Highly shocked clasts in Ilyinets impact breccia, in part, closely resemble clasts seen in Vredefort impact-melt rock (Vredefort Granophyre; for a review, see Reimold and Gibson, 1996).

Breccia samples (for example, suevite I-2, fragmental impact breccia I-1, and impact-melt rocks/breccia I-11, I-12, and I-13) have the following characteristics: In suevite, granitoid-derived clasts are dominant, but a sedimentary clast component is obvious—in contrast to the other two types of impact breccia, where sedimentary clasts are observed far less often. Large clasts in suevite are often low to moderately shocked, whereas clasts within impact-melt fragments from suevite are frequently strongly shock metamorphosed (partially or completely shock melted). Fragmental impact breccia I-4 contains moderately to strongly shocked clasts (multiple sets of PDFs in quartz and feldspar, Table 1).

Clasts in impact-melt breccias are frequently highly shock metamorphosed (*i.e.*, partially to completely shock melted). Textures of Ilyinets impact-melt matrices are variable—from aphanitic to fine-grained crystalline—but most specimens available for this investigation have aphanitic matrices, probably because most of these samples are derived from suevitic breccias. The degree of alteration of these melt rock samples is variable, ranging from nearly unaltered glass to partially or completely devitrified melts, which may be fresh or largely chloritized (*e.g.*, sample I-25).

Shock Metamorphism of Rocks in the Ilyinets Crater

Evidence of shock metamorphism is abundant in rocks and minerals of the Ilyinets impact structure and was described earlier by Masaitis *et al.* (1980), Valter and Ryabenko (1977), Valter and Lazarenko (1982), and Gurov and Gurova (1991b). The discussion of shock metamorphism of the Ilyinets crater in this paper is based on the investigations of cores of drill holes 2100, 5006, 5008, and of some other samples from outcrops in the southern part of the crater (unpublished notebooks, E. G.). Information on the specific samples that were chemically analyzed is given in the previous section and in Table 2.

Shatter cones occur in autochthonous breccias of the crater basement; they rarely occur in boulders and fragments of crystalline

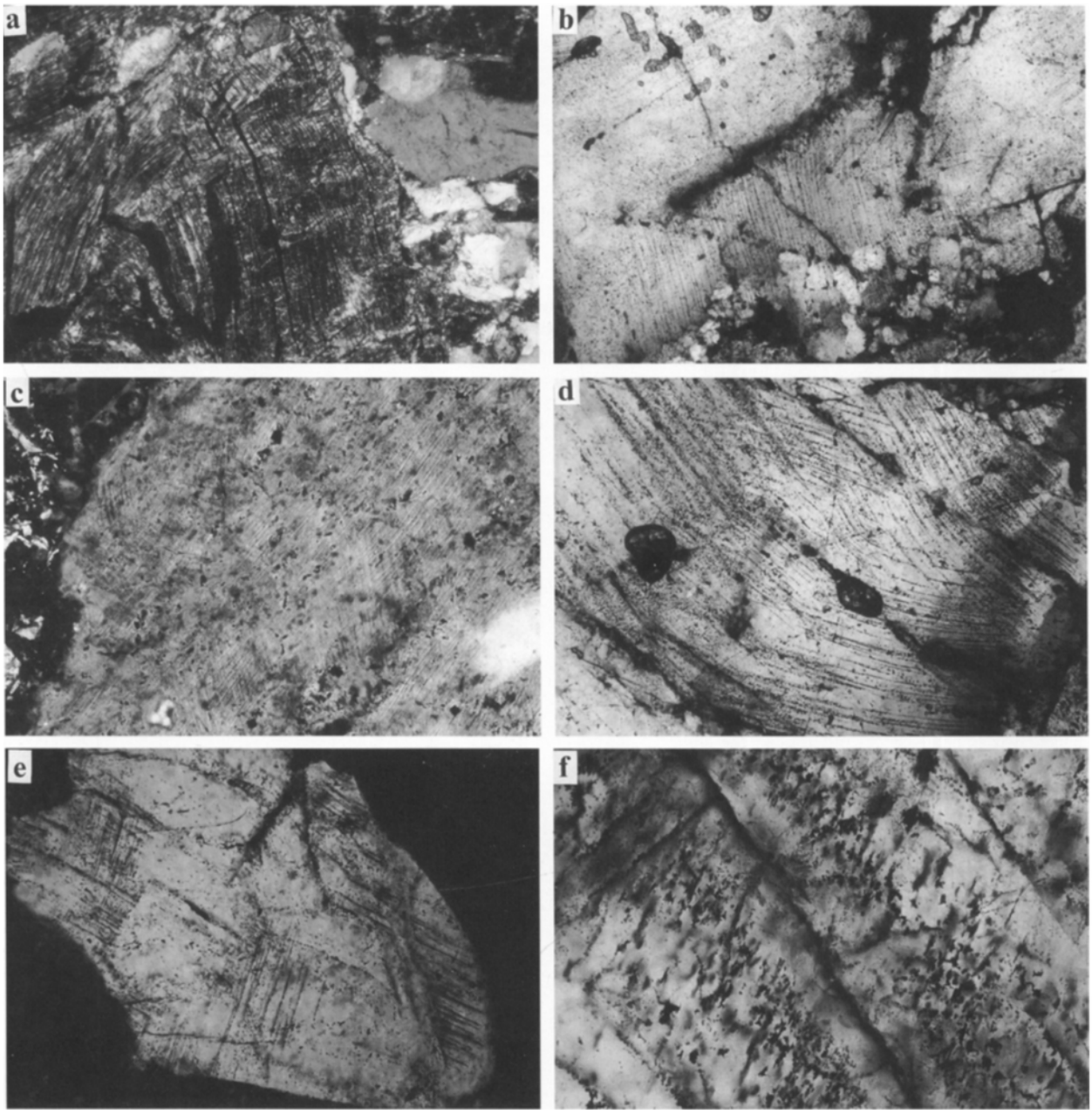

FIG. 6. Microphotographs showing the range of textures and shock metamorphic features observed in Ilyinets target rocks. (a) Kinkbanding in biotite, indicating low-pressure deformation (sample I-26, 1.1 mm wide, crossed polars, gypsum plate). (b) Quartz with two sets of PDFs in centimeter-sized granitic clast (sample I-1, 1.1 mm wide, crossed polars). (c) Potassium feldspar with multiple sets of PDFs in moderately shocked biotite-gneiss clast in sample I-25 (crossed polars, 355 μm wide). (d) Intense shock deformation in quartz from granite fragment I-4 with multiple sets of PDFs (1.1 mm wide, crossed polars). (e) Quartz grain with several sets of PDFs (sample I-25, crossed polars, 1.1 mm wide). (f) Feldspar grain with oxide decoration trails that might represent annealed PDFs (sample I-29, 355 μm wide, crossed polars).

rocks in suevites. They are abundant in drill core samples of core 5008 at depths of 120.0, 152.5, and 166.0 m in suevites and at depth intervals of 270.0–282.4, 300.0–307.2, and 311.0–332.5 m in autochthonous granite breccias. Shock pressures for four individual quartz grains from two granite samples of brecciated basement (Hole 5008, depth 314.0 and 330.0 m) have been determined by the Debye–Scherrer method of Hörz and Quaide (1973) (see also Grieve *et al.*, 1996), yielding pressure estimates of ~8 ± 2 GPa.

Shocked quartz is rare in granites of the brecciated basement, where PDFs have mainly (0001), $\{10\bar{1}3\}$, and $\{10\bar{1}4\}$ orientations (Fig. 4). Basal orientations are common in quartz from brecciated granite (core 5008, 303.0 m). Refractive indices of shocked quartz are slightly decreased with $n_o = 1.551$, $n_e = 1.542$, and birefringence 0.009, corresponding to a shock pressure of ~22 ± 2 GPa (Langenhorst, 1993, 1994; Langenhorst and Deutsch, 1994).

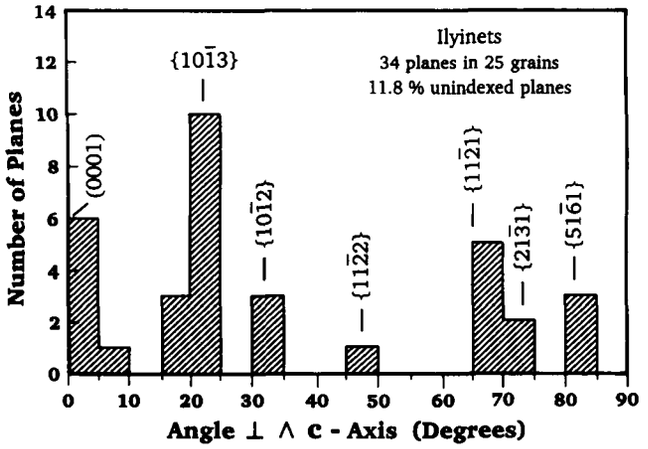

FIG. 7. Crystallographic orientation of PDFs in quartz from shocked clasts in samples I-1, -2, -4, -7, -9, -12, -15, and 16. Histogram shows frequency (number of PDF planes) *vs.* angle between *c*-axis and PDFs; all measurements are plotted (Engelhardt and Bertsch, 1969); the shock-characteristic orientations (0001), {10$\bar{1}$3}, {10$\bar{1}$2}, {11$\bar{2}$2}, {11$\bar{2}$1}, {21$\bar{3}$1}, and {51$\bar{6}$1} are dominating. In addition, information is given on how many planes could be indexed (cf., Grieve *et al.*, 1996).

Quartz in granitic fragments from suevites with low-glass content represents predominantly shock stage Ia of Stöffler (1972), whereas quartz from the suevite matrix rarely contains any evidence of shock metamorphism. Shocked quartz in fragments of crystalline rocks in suevite has undulatory extinction and contains abundant PDFs with several orientations (mainly {10$\bar{1}$3} and {10$\bar{1}$4}, with minor {10$\bar{1}$2}, (0001), and {10$\bar{1}$1}). Refractive indices are lowered to n_o = 1.550 and n_e = 1.540–1.541, with birefringence = 0.008–0.009, indicating shock pressures of ~24 ± 2 GPa (Langenhorst, 1993, 1994; Langenhorst and Deutsch, 1994).

The orientations of PDFs in quartz of the Ilyinets crater are characterized by a fairly common occurrence of the rhombohedral {10$\bar{1}$4} orientation, which has not been indexed in the classical shock-orientation studies (*e.g.*, Engelhardt and Bertsch, 1969; Stöffler and Langenhorst, 1994; Langenhorst, 1994), but has been described in the Russian literature and indexed according to methods of Ansheles (1952). The pole of this system forms an angle of ~18° with the *c*-axis (the theoretical value would be 17° 35') and is different from the pole of the {10$\bar{1}$3} and the {10$\bar{1}$2} systems by 5° and 14°, respectively. This orientation was also found in shocked quartz from other impact craters of the Ukrainian Shield (Gurov and Gurova, 1991b; Gurov *et al.*, 1979) and from the Elgygytgyn impact structure (Gurov and Gurova, 1982). Some of the histograms of PDF orientation in quartz, given by Engelhardt and Bertsch (1969) and Grieve and Alexopoulos (1988), also show a maximum at 18° that is distinct from the {10$\bar{1}$3} peak.

Shock metamorphism of quartz from glass-rich suevites is expressed by undulatory extinction, reduced refractive indices and birefringence, and occurrence of abundant PDFs with multiple orientations per grain (mainly corresponding to the orientations {10$\bar{1}$3} and {10$\bar{1}$4}; see Figs. 4 and 8a–d). The highest level of shock was found in a granite fragment in suevite from hole 5008 at a depth of 68 m. In quartz from this sample, PDF orientations are predominantly {10$\bar{1}$3}, rarely {10$\bar{1}$4} and {10$\bar{1}$2}, whereas (0001) orientations are absent. The refractive indices of quartz from this sample were determined to be n_o = 1.544 and n_e = 1.536, with birefringence = 0.008. These values correspond to shock pressures of 26 ± 2 GPa (references as above). Shocked microcline from the same granite fragment contains abundant PDFs and is characterized by reduced refractive indices: n_g = 1.521, n_p = 1.514, and birefringence = 0.007. These optical properties correspond to a shock pressure of ~15–20 GPa (cf., Stöffler, 1974; Huffman and Reimold, 1996).

There is no indication of diaplectic quartz glass or lechatelierite in samples that indicate shock pressures of more than about 24–26 GPa. These phases seem to have been replaced by fine-grained mosaic aggregates (grain size 10–30 μm) of secondary quartz. Relics of PDFs are rare in such aggregates. The absence of highly shocked quartz and lechatelierite and the scarcity of diaplectic quartz glass are probably due to recrystallization as a result of hydrothermal alteration.

Highly shocked granite and gneiss fragments preserve their initial texture but are composed of cryptocrystalline aggregates of quartz and feldspar. The textures of feldspar grains in these rocks show evidence of partial melting. Often these feldspars are vesicular and contain numerous vesicles ranging from 0.01 to 0.2 mm in diameter. Dark-colored minerals are converted into brown and black cryptocrystalline aggregates of secondary minerals (Fig. 8g).

Impact-melt rocks are dense, fine-grained rocks with numerous inclusions of basement rock and mineral fragments. The inclusion content ranges from ~20 to 40 vol%. The impact-melt rock is dark grey to black in core samples and brown to light brown in surface exposures, probably due to subaerial weathering. The impact-melt rocks contain quartz, feldspar, and mafic minerals in a devitrified glassy matrix (Fig. 8b–e). Feldspar forms oblong prismatic crystallites that are 0.1 to 0.4 mm long and 0.01 to 0.03 mm wide. Fibrous, often sheaf-like, aggregates of feldspar microlites are the main component of the impact melt (Fig. 8g). Feldspar is mainly orthoclase with a low albite content. The main mafic mineral in the melt rock is orthopyroxene that forms acicular to prismatic crystallites ~0.15–0.30 mm long and 0.1 mm wide; however, orthopyroxene is only rarely preserved in the melt rocks but is usually replaced by biotite and chlorite.

Impact glasses occur in suevites as particles and fragments of irregular form and are of grey, greenish-grey, or light brown color. The size of glass inclusions in suevites ranges from ~0.1 mm in the matrix to several centimeters for the largest fragments. Fluidal structures are visible in some samples and in thin sections of glass (Fig. 8e,f). Glasses often contain vesicles (Fig. 8e,f) that are filled with chlorite and clay minerals. Fresh glass is only rarely preserved in the rocks but is commonly devitrified and replaced by secondary minerals, predominantly montmorillonite and chlorite.

Ovoid glass "bombs" (cf., Stähle, 1972) occur in the upper suevite horizon in the southern part of the Ilyinets structure, overlying the impact melt body, or are included in the melt rock. They have a variety of shapes, with sizes ranging from 2 to 10 cm, rarely to 15 cm. Their surface is smooth, and the bombs easily separate from the suevite matrix. Bombs with a diameter of >3–4 cm have a complex structure with crystalline rock cores covered by a glassy crust. The cores are isometric fragments of highly shocked granites and gneisses. The crust comprises zoned devitrified glass ~1 cm thick.

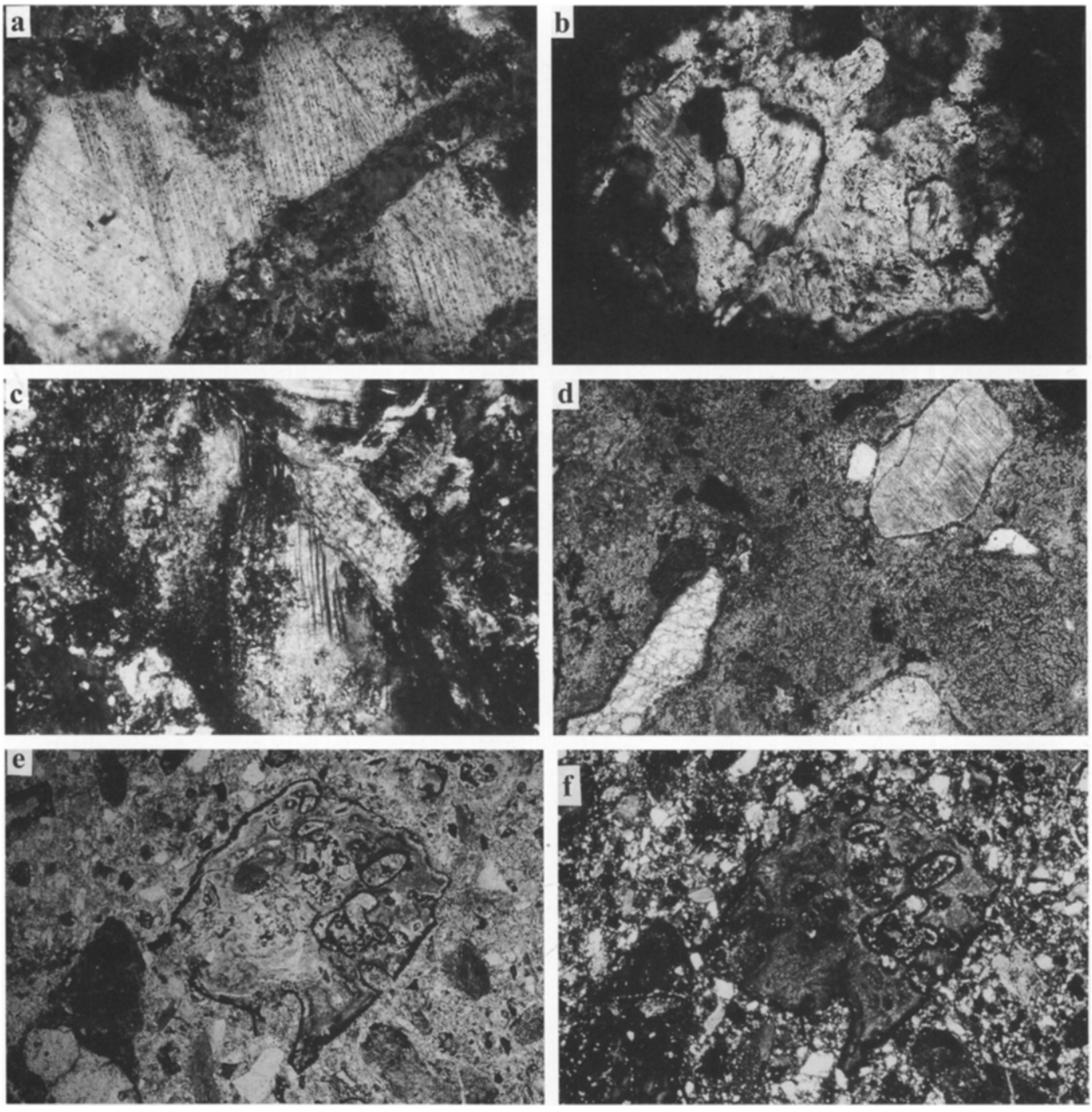

FIG. 8. Microphotographs showing the range of textures and shock metamorphic features observed in Ilyinets impact breccias. (a) Shocked quartz grains with multiple sets of PDFs in gneiss clast from suevite (sample I-25, 565 μm wide, crossed polars, gypsum plate). (b) Glass fragment with quartz clast with multiple sets of PDFs in suevite (sample I-22, 565 μm wide, crossed polars). (c) Largely melted plagioclase clast with melted albite twin lamellae, from biotite gneiss within suevite (sample I-26, 1.1 mm wide, crossed polars). (d) Devitrified impact glass with annealed and shocked quartz clasts (sample I-15, parallel polars, 2.2 mm wide). (e) Devitrified glass fragments (partly chloritized) with flow texture in fine-grained matrix in suevitic breccia (sample I-25, 3.4 mm wide, parallel polars). (f) Same as (e) but with crossed polars.

The zones, 1 to 4 mm thick, differ in their content of mineral inclusions and color.

Impact-induced high-pressure phases in the rocks from the Ilyinets structure include coesite and diamond. Only low concentrations of coesite were found by x-ray diffractometry of acid dissolution residues of granite fragments shocked to ~15 GPa (Gurov *et al.*, 1980). Impact diamonds are present in some impact-melt rocks of the Ilyinets crater. The shape and size of diamond grains are similar to those of graphite from granites and gneisses of the crater basement, which indicates shock transformation of graphite into diamond (similar to the formation of impact diamonds at the Popigai impact structure; *e.g.*, Masaitis *et al.*, 1972; Koeberl *et al.*, 1997a). The transition from graphite with a density of ~2.2 g/cm^3 to diamond with a density of ~3.5 g/cm^3 is accompanied by a decrease in volume of a factor of 1.6. Diamond grains are anisotropic and their birefringence ranges from 0.003 to 0.018. The phase composition of impact diamond was studied using x-ray diffractometry, which indicates that the grains are polycrystalline aggregates. The x-ray diffraction patterns suggest the presence of both cubic and hexagonal diamond structure (see Koeberl *et al.*, 1997a, for a

FIG. 8. *Continued.* (g) Spherulitic devitrification texture of glass between strongly annealed relic grains (relics of mafic precursor minerals are clusters of opaque phases) (sample I-29, 3.4 mm wide, crossed polars).

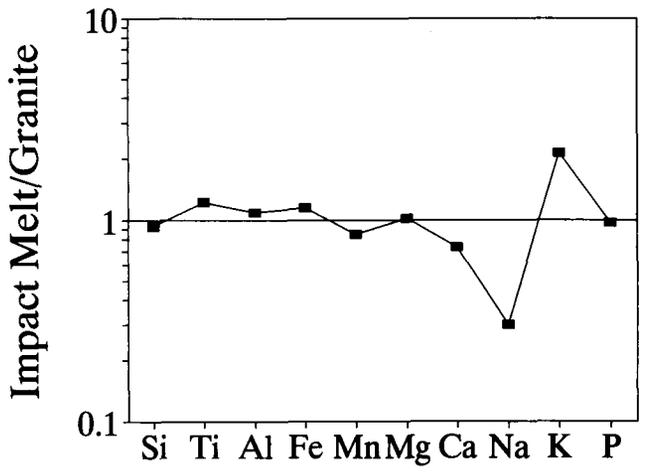

FIG. 9. Comparison of average impact-melt breccia composition and average target granite composition (data from Tables 4 and 5).

discussion of the problems with identification of these phases by XRD). The properties of the impact diamonds from the Ilyinets structure are similar to properties of diamond from the Zapadnaya crater (Gurov *et al.*, 1996).

Chemistry of Target Rocks and Impactites of the Ilyinets Structure

Average major element abundances, determined by classical wet chemical methods (E. G., unpubl. data), of granitoids and impact-melt rocks are given in Table 3. From major element wet chemical data (Masaitis *et al.*, 1980; Valter and Ryabenko, 1977), the relative abundance of the crater basement rocks was calculated to be granite (80%,) gneiss (15%), and amphibolite (5%). The mean composition of impact-melt rock (Masaitis *et al.*, 1980; Valter and Ryabenko, 1977) was compared with data for target granitoids (Table 3), showing similar compositions.

To provide additional chemical data for Ilyinets, we determined the major and trace element composition of 31 target rocks and impactite samples. The results of these analyses are given in Table 4 for target granitoids and in Table 5 for impactites and clasts therein. The average major element composition of the granitoids given in Table 4 is very similar to data mentioned above (Table 3), which indicates a fairly uniform composition of basement granitoids. Also, the composition of impact-melt rocks shows only limited variation (Table 5). A comparison of the target granitoid composition and the average impact-melt rock composition (calculated from those samples in Table 5 that are listed either as impact glass or impact melt breccia) is shown in Fig. 9 and clearly indicates that only the alkali elements, Na and K, have anomalous abundances.

TABLE 3. Average major element data for Ilyinets granitoids and impact-melt rock.

	Granitoids (27)	Impact melt (4)
SiO_2	65.67	65.77
TiO_2	0.31	0.50
Al_2O_3	14.60	15.68
Fe_2O_3	5.79	3.44
MnO	0.09	0.04
MgO	2.46	1.33
CaO	1.99	1.30
Na_2O	2.93	1.12
K_2O	4.49	9.59
Total	98.33	97.47

Data in wt%, obtained by wet chemical analysis.
All Fe as Fe_2O_3.

Our data allow comparison of trace element compositions in target rocks and impactites. Figure 10 shows several chondrite-normalized rare earth element (REE) diagrams. Although the major element composition of the granites seems fairly constant, the REE patterns show some interesting variations, with different slopes mainly in the light REE region and slight variations in the extent of the negative Eu anomaly (Fig. 10a). The impact-melt breccias show a much more homogeneous REE composition, but the extent of the Eu anomaly is still variable (Fig. 10b). Suevites and clasts within suevites, as well as the sedimentary rock fragment from location I-4-15, show identical REE patterns, but with absolute concentrations that vary by a factor of five (Fig. 10c). The relatively high, heavy REE content of the sample from location I-6-8 could be due to admixture of some siltstone. Of the other target rocks, the amphibolite shows a distinctly different trace element composition (Table 4) and REE pattern (Fig. 10d). Admixture of a small amphibolite component with an almost flat pattern is in agreement with slightly lower slopes of REE patterns in impact-melt rocks as compared to granitoids and is in keeping with the major element calculations mentioned above.

Comparison of the average impact-melt rock and target rock siderophile element abundances shows very minor enrichments in Cr and Ni in the melt rocks, but no significant difference in the Co content. However, a few of the impact-melt breccias have fairly high Ir contents (~1 ppb), which is significantly higher than the detection limit (mostly 0.5 ppb in these samples). Thus, the data suggest that a minor meteoritic component is present in some of the impact-melt breccias. Earlier attempts by Valter and Ryabenko (1977) and G. Kolesov (in Feldman, 1982, and Gurov and Gurova, 1991b) did not yield a clear result either—one of these studies concluded that an iron meteorite was involved; the other, a stony projectile.

The main heterogeneity of impact-melt rocks is in the content of K and Na. The upper part of the impact-melt rock body is enriched in K, not only in comparison with its content in basement rocks, but

TABLE 4. Chemical composition of granitoids from the Ilyinets impact structure.

Sample	I-1	I-2	I-3	I-4	I-5	I-6	I-31	I-29	I-30	I-7	I-25	I-8	Granite	
Location	5008-215m	5008-279m	5008-314m	5008-330m	18480-160m	18480-215m	Q.-I-12	Q.-I-6-50	Q.-I-9-1	2100-311m	Q.-I-4-12	18480-178m	Average	Range
Rock type	Granite	Granite	Granite	Granitic breccia	Granite	Granite	Granite	Granite clast	Biotite granite cl.	Biotite gneiss	Biotite gneiss clast	Amphibolite		
SiO_2	69.24	67.72	69.08	69.43	72.52	71.01	62.36	60.15	70.70	56.52	58.29	47.92	69.83 ± 1.54	67.72–72.52
TiO_2	0.18	0.21	0.21	0.46	0.17	0.21	0.59	0.05	0.61	0.37	1.62	0.42	0.24 ± 0.10	0.17–0.46
Al_2O_3	14.83	14.53	14.40	14.74	14.02	14.47	16.37	13.83	13.70	14.64	12.63	14.81	14.50 ± 0.26	14.02–14.83
Fe_2O_3	3.45	3.01	3.13	3.37	1.61	2.74	7.11	12.18	4.27	8.34	9.96	13.57	2.88 ± 0.62	1.61–3.45
MnO	0.06	0.04	0.03	0.06	0.02	0.02	0.06	0.23	0.03	0.14	0.07	0.22	0.04 ± 0.02	0.02–0.06
MgO	1.73	1.47	1.54	2.22	0.67	0.88	1.54	0.03	1.19	7.53	3.96	8.19	1.42 ± 0.52	0.67–2.22
CaO	0.36	1.49	0.96	0.38	1.62	1.87	4.21	0.38	1.75	1.36	1.41	9.15	1.11 ± 0.59	0.36–1.87
Na_2O	3.98	2.86	4.39	4.52	2.89	2.98	4.44	1.72	3.26	2.49	0.80	2.07	3.60 ± 0.71	2.86–4.52
K_2O	4.67	6.51	3.72	2.71	5.63	4.21	1.72	8.99	2.96	2.54	6.49	0.52	4.57 ± 1.24	2.71–6.51
P_2O_5	0.13	0.05	0.16	0.09	0.12	0.10	0.42	0.19	0.02	0.71	0.91	0.10	0.11 ± 0.04	0.05–0.16
L.O.I.	1.37	1.80	1.40	2.02	0.41	0.54	0.93	2.01	1.12	5.18	3.29	2.50	1.26 ± 0.60	0.41–2.02
Total	100.00	99.69	99.02	99.99	99.67	99.04	99.75	99.76	99.61	99.81	99.43	99.46	99.57	–
Sc	5.56	4.49	4.19	4.42	2.67	4.74	10.2	1.85	5.63	19.9	16.1	44.6	4.35 ± 0.86	2.67–5.56
V	36	62	66	54	34	44	95	25	50	142	188	357	49 ± 12	34–66
Cr	12.9	42.6	21.6	15.8	12.7	15.3	7.38	14.4	71.2	278	52.3	162	20.2 ± 10.5	12.7–42.6
Co	38.3	21.6	31.2	31.6	28.8	44.3	15.3	21.3	9.56	31.4	21.8	72.9	32.6 ± 7.2	21.6–44.3
Cu	4	2	4	6	8	6	31	42	39	5	55	64	5 ± 2	2–8
Ni	22	27	22	22	19	26	39	30	2	36	27	87	23 ± 3	19–27
Zn	41	70	92	57	30	39	106	122	78	240	85	133	55 ± 21	30–92
Ga	20	12	14	15	14	8	23	18	23	33	20	28	14 ± 4	8–20
As	0.55	0.15	0.49	0.52	0.58	0.05	0.21	1.22	0.31	0.54	0.86	0.32	0.39 ± 0.21	0.05–0.58
Se	0.14	0.18	0.12	0.15	0.09	0.14	0.17	0.25	0.16	0.14	0.13	0.07	0.14 ± 0.03	0.09–0.18
Br	0.38	0.36	0.27	0.27	0.57	0.41	0.09	0.08	0.05	0.41	0.05	0.5	0.38 ± 0.10	0.27–0.57
Rb	135	180	116	119	168	167	108	222	182	184	305	10	148 ± 25	116–180
Sr	205	254	256	153	330	350	387	286	263	125	81	56	258 ± 68	153–350
Y	13	10	15	13	15	15	30	90	6	36	31	23	14 ± 2	10–15
Zr	98	190	180	250	110	120	120	60	178	290	301	87	158 ± 54	98–250
Nb	14	13	14	12	11	15	11	4	22	17	23	7	13 ± 1	11–15
Ag	0.07	0.08	0.03	0.03	0.02	0.02	0.05	0.18	0.06	0.04	0.15	0.03	0.04 ± 0.02	0.02–0.08
Sb	0.05	0.051	0.087	0.13	0.06	0.03	0.032	0.17	0.21	0.05	0.17	0.06	0.07 ± 0.03	0.03–0.13
Cs	1.08	1.11	1.04	0.88	0.85	1.32	0.92	0.29	1.38	2.58	2.35	0.11	1.05 ± 0.16	0.85–1.32
Ba	845	1070	572	385	1180	820	235	1670	657	1270	3580	58	812 ± 272	385–1180
La	37.4	65.5	11.5	100	32.6	15.4	51.1	24.1	18.3	31.2	34.5	4.67	43.7 ± 30.7	11.5–100.0
Ce	69.5	117	21.8	219	56.3	35.2	93.6	40.8	32.7	59.9	74.1	10.3	86.5 ± 66.5	21.8–219
Nd	32.2	52.8	11.4	90.1	28.9	15.9	50.5	22.5	16.8	35.3	52.4	7.88	38.6 ± 26.6	11.4–90.1
Sm	4.82	8.15	2.92	9.62	4.91	2.57	10.9	4.82	2.44	9.09	13.1	2.81	5.50 ± 2.58	2.57–9.62
Eu	0.85	1.01	0.69	0.94	0.99	0.93	1.43	1.58	0.92	1.48	1.93	0.92	0.90 ± 0.11	0.69–1.01
Gd	4.8	5.8	3.56	6.6	5.3	3.2	9.37	5.9	2.88	10.2	12.8	3.31	4.88 ± 1.19	3.20–6.60
Tb	0.55	0.59	0.48	0.79	0.6	0.51	1.35	0.93	0.38	1.36	1.44	0.63	0.59 ± 0.10	0.48–0.79
Tm	0.15	0.12	0.19	0.24	0.22	0.23	0.49	0.33	0.18	0.45	0.51	0.37	0.19 ± 0.04	0.12–0.24
Yb	0.65	0.64	0.99	0.99	1.15	1.08	2.57	2.14	0.83	2.81	2.75	2.28	0.92 ± 0.20	0.64–1.15
Lu	0.078	0.088	0.12	0.12	0.13	0.13	0.34	0.33	0.11	0.41	0.36	0.38	0.11 ± 0.02	0.08–0.13
Hf	2.45	5.08	5.58	6.92	2.83	2.78	3.28	0.071	5.84	9.19	8.37	1.61	4.27 ± 1.68	2.45–6.92

TABLE 4. *Continued.*

Sample	I-1	I-2	I-3	I-4	I-5	I-6	I-31	I-29	I-30	I-7	I-25	I-8	Granite	
													Average	Range
Location	5008-215m	5008-279m	5008-314m	5008-330m	18480-160m	18480-215m	Q.-I-12	Q.-I-6-50	Q.-I-9-1	2100-311m	Q.-I-4-12	18480-178m		
Rock type	Granite	Granite	Granite	Granitic breccia	Granite	Granite	Granite	Granite clast	Biotite granite cl.	Biotite gneiss	Biotite gneiss clast	Amphibolite		
Ta	1.07	0.95	0.88	0.86	0.62	1.02	0.93	0.048	0.99	1.17	1.19	0.15	0.90 ± 0.15	0.62–1.07
W	n.d.	n.d.	n.d.	n.d.	n.d.	n.d.	0.4	0.2	0.4	n.d.	0.51	n.d.	n.d.	–
Ir (ppb)	<1	<1	<1	<2	<2	<2	<1.5	0.8	0.9	<2	<1.5	<2	<1	–
Au (ppb)	<1	0.3	0.6	<1	<1	0.2	45	43	1.5	1.5	50	<1	0.2 ± 0.2	0.0–0.6
Hg	0.03	0.04	0.05	0.04	0.04	0.07	0.11	0.07	0.08	0.06	0.05	0.04	0.05 ± 0.01	0.03–0.07
Th	23.9	42.3	1.86	70.4	16.6	9.34	7.29	2.04	10.5	11.2	28.9	0.19	27.4 ± 23.0	1.9–70.4
U	2.16	2.42	2.09	1.91	2.39	0.96	2.58	0.85	0.91	7.12	4.54	0.09	1.99 ± 0.49	0.96–2.42
K/U	18029	22417	14833	11806	19630	36545	5556	88137	27106	2973	11913	48148	20543 ± 7913	11806–36545
Th/U	11.06	17.48	0.89	36.86	6.95	9.73	2.83	2.40	11.54	1.57	6.37	2.11	13.8 ± 11.4	0.9–36.9
Zr/Hf	40.0	37.4	32.3	36.1	38.9	43.2	36.6	845.1	30.5	31.6	36.0	54.0	38.0 ± 3.4	32.3–43.2
Hf/Ta	2.29	5.35	6.34	8.05	4.56	2.73	3.53	1.48	5.90	7.85	7.03	10.73	4.89 ± 1.99	2.29–8.05
La/Th	1.56	1.55	6.18	1.42	1.96	1.65	7.01	11.81	1.74	2.79	1.19	24.58	2.39 ± 1.71	1.42–6.18
La_N/Yb_N	38.88	69.16	7.85	68.26	19.16	9.64	13.44	7.61	14.90	7.50	8.48	1.38	35.5 ± 25.6	7.85–69.16
Eu/Eu*	0.54	0.45	0.65	0.36	0.59	0.99	0.43	0.91	1.06	0.47	0.46	0.92	0.60 ± 0.20	0.36–0.99

Major element data in wt%, trace element data in ppm, except as noted. All Fe as Fe_2O_3. cl. = Clast. Numbers given under sample location are either quarry numbers or drill core numbers with depths in meters.

also relative to the composition of the underlying impact-melt rocks. Potassium enrichments are also observed in inclusions of crystalline rocks in the upper horizon of the melt body and in overlying suevites (Gurov and Gurova, 1991b; Masaitis *et al.*, 1980; Valter and Ryabenko, 1977). High K and low Na values occur commonly in impact-melt rocks, for example, Brent (Grieve, 1978), Boltysh (Gurov and Gurova, 1991b; Gurov *et al.*, 1986), and Ames (Koeberl *et al.*, 1997b). Although some authors (*e.g.*, Valter and Ryabenko, 1977; Yakovlev *et al.*, 1982) explain the enrichment in K by vaporization processes, mobilization of the alkali elements in postimpact hydrothermal systems is much more likely (cf., Koeberl *et al.*, 1997b). Considering the evidence for hydrothermal alteration in Ilyinets impactites, this mechanism seems to have dominated in the case of the Ilyinets structure.

The K/Ar age of two bulk samples of clast-free impact melt was determined by A. K. Boiko (pers. comm. to E. P. Gurov, 1997) and yielded ~390 Ma (sample location I-4) and 410 Ma (drill hole 2100, 255 m depth). These data agree with earlier K-Ar studies of Ilyinets impact-melt rocks that yielded ages of ~395–400 Ma (Nikolsky, 1975).

DISCUSSION AND CONCLUSIONS

The Ilyinets impact crater formed in the Precambrian crystalline basement of the Ukrainian Shield. Proterozoic granites and gneisses are the main rock types in the target area. Occurrence of the sedimentary rock fragments in suevites and breccias indicates that a sedimentary cover was present on the crystalline basement surface before the impact (Fig. 5). These sediments are not preserved in their initial position; thus, their thickness and age are unknown. The relatively high content of sedimentary rock fragments in suevites indicates a thickness of the cover of a few tens of meters.

The Ilyinets impact structure is now eroded down to the surface of autochthonous rocks. Preservation of postimpact sediments at a distance of ~3 km from the crater center indicates that the minimal diameter of the apparent crater floor to the base of the rim was ~6 km. The original rim-to-rim diameter of the structure was estimated to be ~7–7.5 km (Gurov and Gurova, 1991b). Using the equations given by Melosh (1989), the depth of a complex crater 7.5 km in diameter is ~550 m (Gurov *et al.*, 1995a,b). Thus, the depth of erosion of the Ilyinets structure since formation is estimated at ~250 m (Fig. 5).

Glass bombs are common in the upper horizon of the suevites on top of the impact-melt layer. This suevite horizon formed by fallback of material ejected from the crater. Preservation of the bombs and their distinct contact with suevite indicate that they fell in a solid state. The thickness of the fallback suevites is to ~10 m in quarries in the southern part of the structure; these rocks compose about one-tenth of the total thickness of allochthonous rocks in this area of the Ilyinets structure. This ratio may not represent the pre-erosional thickness before partial erosion by the Sobik river.

Shock metamorphosed rocks and minerals are common in rocks from the Ilyinets structure, mainly in the form of quartz and feldspar clasts with several sets of PDFs with distinct crystallographic orientations. Coesite and impact diamond occur in breccias and impact-melt rocks but are rare. Quartz and feldspar shocked to >26 GPa is very rare; we observed some diaplectic quartz glass (30–35 GPa), evidence for partial shock melting (35–45 GPa), and bulk shock melting (>45 GPa). Most strongly shocked clasts seem to have recrystallized into fine-grained aggregates of secondary quartz and feldspars, either as a result of slow cooling or postimpact hydrothermal activity.

TABLE 5. Chemical composition of impactites and clasts from the Ilyinets impact structure.

Sample	I-22	I-23	I-24	I-26	I-27	I-9	I-10	I-11	I-12	I-13	I-14	I-15	I-16	I-17	I-18	I-19	I-20	I-21	I-28	Impact melt	
Location	Q.-I-2	Q.-I-2-46-CL	Q.-I-2-46-rim	Q.-I-4-13	Q.-I-4-15	18480-5 m	18480-15 m	18480-29 m	18480-35 m	18480-38 m	2100-36 m	Q.-I-6	Q.-I-9	Q.-I-2	Q.-I-18	Q.-I-2	Q.-I-2	Q.-I-2	Q.-I-6-8	Average	Range
Rock type	Suevite	Granite Cl./Suevite	Rim of clast	Suevite	Siltstone cl./Suevite	Impact breccia	Suevite(?)	Impact melt br.	Impact melt br.	Impact melt br.	Impact glass	Impact glass	Impact glass	Impact glass	Impact glass	Impact glass	Impact glass	Impact melt br.	Impact melt br.		
SiO_2	64.73	69.86	64.70	63.88	57.26	61.03	58.94	64.31	63.40	62.45	65.15	62.12	63.55	62.85	66.68	66.84	66.30	65.34	63.61	64.45 ± 1.63	62.12–66.84
TiO_2	0.47	0.26	0.53	0.52	0.59	0.24	0.34	0.23	0.24	0.25	0.25	0.55	0.27	0.54	0.24	0.22	0.23	0.19	0.51	0.29 ± 0.12	0.19–0.55
Al_2O_3	14.82	13.13	14.93	14.30	13.80	14.98	13.94	15.26	14.75	15.59	16.50	15.56	18.22	15.08	15.26	15.63	15.57	16.67	15.11	15.83 ± 0.93	14.75–18.22
Fe_2O_3	4.58	3.28	4.27	5.29	9.83	5.38	9.90	4.32	4.58	4.07	3.02	4.64	1.31	4.96	3.69	2.12	1.87	2.06	5.05	3.33 ± 1.24	1.31–4.96
MnO	0.04	0.01	0.01	0.04	0.04	0.05	0.06	0.07	0.08	0.03	0.03	0.03	0.01	0.03	0.03	0.02	0.01	0.02	0.14	0.03 ± 0.02	0.01–0.08
MgO	1.00	0.14	0.10	0.77	1.56	3.47	3.86	3.28	3.12	2.95	1.70	1.46	0.31	1.09	1.58	0.18	0.10	0.10	0.87	1.44 ± 1.17	0.10–3.28
CaO	0.26	0.30	0.34	0.42	0.76	0.77	2.16	1.07	1.12	0.46	0.42	0.50	0.54	0.51	3.30	0.38	0.33	0.36	0.34	0.82 ± 0.83	0.33–3.30
Na_2O	0.25	0.67	0.32	0.16	0.39	1.76	2.25	1.55	1.84	0.55	1.16	0.67	0.59	0.80	2.83	0.41	0.42	1.11	0.51	1.08 ± 0.71	0.41–2.83
K_2O	9.89	8.82	11.09	10.10	7.27	8.06	3.86	6.22	6.19	10.74	9.47	11.33	12.23	10.93	3.60	12.44	12.77	12.18	11.04	9.83 ± 2.96	3.60–12.77
P_2O_5	0.04	0.04	0.05	0.07	0.13	0.18	0.08	0.14	0.14	0.15	0.12	0.16	0.04	0.17	0.16	0.05	0.03	0.03	0.13	0.11 ± 0.06	0.03–0.17
L.O.I.	3.61	2.57	2.72	3.86	7.87	4.10	4.47	3.68	3.62	2.45	2.23	3.52	2.39	3.70	2.52	1.80	1.99	1.20	2.69	2.64 ± 0.82	1.20–3.70
Total	99.69	99.08	99.06	99.41	99.50	100.01	99.86	100.11	99.08	99.68	100.05	100.53	99.45	100.66	99.89	100.09	99.62	99.24	100.00	99.85	–
Sc	11.8	6.13	10.7	9.32	16.3	11.1	21.4	9.99	10.8	11.2	9.85	9.94	10.7	10.9	10.9	7.72	7.88	3.43	10.4	9.39 ± 2.20	3.43–11.2
V	91	50	65	75	102	96	129	85	84	95	87	76	108	90	88	65	59	41	73	80 ± 18	41–108
Cr	64.5	44.6	65.5	65.1	83.5	59.9	47.5	61.8	65.9	71.1	55.1	79.3	81.1	85.1	66.2	46.8	57.1	36.4	95.1	64.2 ± 14.2	36.4–85.1
Co	17.9	7.27	9.98	16.5	32.1	40.4	27.5	28.9	30.1	25.1	33.3	35.7	25.6	11.1	53.5	17.1	24.6	54.1	51.6	30.8 ± 12.7	11.1–54.1
Ni	67	30	60	60	100	15	18	31	33	40	45	36	40	13	40	52	28	32	260	35 ± 10	13–52
Cu	41	13	15	19	30	40	28	36	42	40	35	54	77	21	38	35	30	30	32	40 ± 14	21–77
Zn	75	34	38	43	96	83	105	70	86	85	108	220	65	33	70	62	29	199	73	93 ± 59	29–220
Ga	13	15	12	19	15	15	32	7	5	32	9	12	24	17	25	9	26	7	16	16 ± 9	5–32
As	0.46	0.82	1.49	0.83	4.27	0.09	0.23	0.35	0.22	0.19	0.77	0.55	1.21	0.98	0.48	0.32	0.66	0.46	0.41	0.56 ± 0.31	0.19–1.21
Se	0.09	0.21	0.16	0.07	0.21	0.08	0.19	0.07	0.09	0.12	0.08	0.05	0.12	0.09	0.08	0.08	0.05	0.11	0.12	0.09 ± 0.02	0.05–0.12
Br	0.16	0.22	0.19	0.11	0.12	0.39	0.16	0.52	0.26	0.49	0.081	0.34	0.36	0.23	0.11	0.31	0.38	0.45	0.12	0.32 ± 0.14	0.08–0.52
Rb	219	201	195	198	205	199	227	223	223	219	202	226	210	230	155	191	205	275	203	214 ± 28	155–275
Sr	58	94	128	59	132	105	190	190	220	131	87	103	93	134	330	110	128	270	146	163 ± 76	87–330
Y	23	10	24	14	43	16	15	19	20	21	23	23	28	19	21	30	18	17	40	22 ± 4	17–30
Zr	162	110	158	149	146	165	190	190	195	160	100	140	120	155	155	185	195	120	186	156 ± 32	100–195
Nb	14	15	15	14	15	27	36	12	12	14	14	15	15	17	15	16	14	8	15	14 ± 2	8–17
Ag	0.04	0.11	0.075	0.054	0.15	0.06	0.03	0.04	0.05	0.04	0.03	0.03	0.03	0.036	0.05	0.05	0.093	0.07	0.043	0.047 ± 0.02	0.030–0.093
Sb	0.15	0.11	0.08	0.079	0.11	0.04	0.03	0.04	0.05	0.02	0.03	0.015	0.087	0.095	0.88	0.029	0.066	0.036	0.068	0.12 ± 0.24	0.02–0.88
Cs	1.02	0.73	0.61	0.66	0.51	0.72	1.03	0.82	0.84	0.87	0.31	0.47	0.37	0.54	0.83	0.36	0.54	0.58	0.69	0.59 ± 0.20	0.31–0.87
Ba	662	853	733	615	412	635	315	830	776	730	660	690	593	670	685	690	720	1770	1690	801 ± 312	593–1770
La	47.2	27.9	55.8	43.9	146	26.5	48.2	23.6	20.4	33.3	19.8	43.3	62.5	33.9	32.2	54.1	48.9	10.6	87.4	34.8 ± 15.3	10.6–62.5
Ce	84.1	51.7	94.7	72.8	247	55.2	86.4	62.1	51.3	63.2	48.7	93.4	120	73.4	59.8	124	84.7	20.3	157	72.8 ± 29.5	20.3–124
Nd	42.2	25.7	48.1	35.1	118	26.3	42.4	28.4	24.4	31.2	24.7	44.6	57.9	34.8	26.5	61.1	39.7	11.7	76.9	35.0 ± 14.2	11.7–61.1
Sm	7.85	4.78	8.85	6.25	18.4	4.54	5.95	3.17	3.18	6.03	4.09	6.39	10.5	4.87	5.02	9.11	6.33	1.76	13.2	5.50 ± 2.47	1.76–10.5
Eu	1.56	0.73	1.72	1.09	3.29	0.91	0.59	0.95	0.95	1.01	0.97	1.31	1.38	1.19	0.95	1.86	1.11	0.96	2.01	1.15 ± 0.27	0.95–1.86
Gd	8.67	4.6	9.2	6.36	14.7	4.95	4.7	4.2	3.6	6.1	4.9	5.9	8.2	5.1	5.9	10.7	5.5	2.1	10.1	5.65 ± 2.18	2.10–10.70
Tb	0.91	0.43	1.03	0.62	1.76	0.66	0.55	0.58	0.57	0.73	0.69	0.82	1.07	0.67	0.65	1.19	0.66	0.33	1.31	0.72 ± 0.23	0.33–1.19
Tm	0.41	0.19	0.45	0.25	0.68	0.27	0.22	0.23	0.27	0.32	0.28	0.31	0.37	0.27	0.23	0.34	0.29	0.18	0.51	0.28 ± 0.05	0.18–0.37
Yb	1.98	1.01	2.37	1.45	4.09	1.43	0.96	1.41	1.44	1.52	1.65	1.58	1.72	1.41	1.21	1.79	1.44	1.06	2.86	1.48 ± 0.20	1.06–1.79
Lu	0.24	0.14	0.34	0.21	0.58	0.19	0.15	0.18	0.21	0.18	0.2	0.21	0.21	0.19	0.16	0.23	0.19	0.15	0.39	0.19 ± 0.02	0.15–0.23
Hf	4.29	3.17	4.83	4.19	4.13	3.41	6.26	3.81	3.79	4.49	3.83	4.43	4.51	4.73	3.65	4.05	5.26	2.46	4.98	4.09 ± 0.70	2.46–5.26
Ta	0.82	0.79	0.98	0.83	0.73	0.73	1.91	0.73	0.75	0.94	0.68	0.78	0.89	0.82	0.81	0.74	0.87	0.44	0.79	0.77 ± 0.13	0.44–0.94

TABLE 5. *Continued.*

Sample	I-22	I-23	I-24	I-26	I-27	I-9	I-10	I-11	I-12	I-13	I-14	I-15	I-16	I-17	I-18	I-19	I-20	I-21	I-28	Impact melt	
Location	Q.-I-2	Q.-I-2-46-CL	Q.-I-2-46-rim	Q.-I-4-13	Q.-I-4-15	18480-5 m	18480-15 m	18480-29 m	18480-35 m	18480-38 m	2100-36 m	Q.-I-6	Q.-I-9	Q.-I-2	Q.-I-18	Q.-I-2	Q.-I-2	Q.-I-2	Q.-I-6-8	Average	Range
Rock type	Suevite	Granite Cl/Suevite	Rim of clast	Suevite	Siltstone cl./Suevite	Impact breccia	Suevite(?)	Impact melt br.	Impact melt br.	Impact melt br.	Impact glass	Impact glass	Impact glass	Impact glass	Impact glass	Impact glass	Impact glass	Impact melt br.	Impact melt br.		
W	0.43	0.45	0.59	0.47	0.65	n.d.	n.d.	n.d.	n.d.	n.d.	n.d.	n.d.	n.d.	n.d.	n.d.	n.d.	n.d.	n.d.	1.04	–	–
Ir (ppb)	<1	<2	<1.5	1	<2	<1	<2	0.9	0.9	<1	<1	0.7	<1	1.2	1.1	0.49	0.61	<1	<1.5	0.84 ± 0.24	0–1.2
Au (ppb)	13	13	27	19	28	0.8	0.5	0.9	0.8	4.5	1	2.8	1.3	0.6	0.4	0.7	0.6	0.8	25	1.31 ± 1.18	0.40–4.50
Hg	0.02	0.04	0.03	0.11	0.034	0.09	0.05	0.06	0.07	0.07	0.02	0.061	0.05	0.09	0.05	0.08	0.03	0.04	0.03	0.06 ± 0.02	0.02–0.09
Th	15.5	20.2	18.5	16.8	12.6	9.84	29.9	16.9	14.1	14.7	14.2	22.9	29.7	22.1	16.1	28.4	26.8	2.62	30.3	19.0 ± 7.6	2.6–29.7
U	1.67	1.21	2.71	2.09	4.25	1.58	1.43	0.79	0.87	2.51	1.55	1.52	2.55	1.21	1.81	1.12	2.11	0.49	2.31	1.50 ± 0.66	0.49–2.55
K/U	49351	60744	34102	40271	14255	42511	22494	65612	59291	35647	50914	62094	39980	75248	16575	92560	50434	207126	39827	68680 ± 47863	16575–207126
Th/U	9.28	16.69	6.83	8.04	2.96	6.23	20.91	21.39	16.21	5.86	9.16	15.07	11.65	18.26	8.90	25.36	12.70	5.35	13.12	13.63 ± 6.06	5.35–25.36
Zr/Hf	37.8	34.7	32.7	35.6	35.4	48.4	30.4	49.9	51.5	35.6	26.1	31.6	26.6	32.8	42.5	45.7	37.1	48.8	37.3	38.9 ± 8.8	26.1–51.5
Hf/Ta	5.23	4.01	4.93	5.05	5.66	4.67	3.28	5.22	5.05	4.78	5.63	5.68	5.07	5.77	4.51	5.47	6.05	5.59	6.30	5.35 ± 0.44	4.51–6.05
La/Th	3.05	1.38	3.02	2.61	11.59	2.69	1.61	1.40	1.45	2.27	1.39	1.89	2.10	1.53	2.00	1.90	1.82	4.05	2.88	1.98 ± 0.71	1.39–4.05
La_N/Yb_N	16.11	18.67	15.91	20.46	24.12	12.52	33.93	11.31	9.57	14.80	8.11	18.52	24.55	16.25	17.98	20.42	22.95	6.76	20.65	15.6 ± 5.7	6.8–24.6
Eu/Eu*	0.58	0.48	0.58	0.53	0.61	0.59	0.34	0.80	0.86	0.51	0.66	0.65	0.45	0.73	0.53	0.58	0.57	1.53	0.53	0.72 ± 0.28	0.45–1.53

Major element data in wt%, trace element data in ppm, except as noted. All Fe as Fe_2O_3. cl. = clast; br. = breccia. Numbers given under sample location are either quarry numbers or drill core numbers with depths in meters.

Impact-melt rocks occur as a coherent layer in the southern part of the structure and as a complex system of dike-like bodies in suevites. The chemical composition of impact-melt breccias is similar to the average composition of granites and gneisses of the crater basement. Enrichment in K of the upper horizon of the melt body is due to its high mobility in the high-temperature melts and postimpact hydrothermal fluids. There is some evidence for the presence of an extraterrestrial component in a few of the impact-melt rock samples, as indicated by slight enrichments in the siderophile element abundances, including Ir. The K-Ar whole-rock age of impact melt of the crater is 385–410 Ma, which is in agreement with the previously determined palynological age of the crater-fill sediments, which yielded an early Devonian age.

Further work on Ilyinets is necessary to confirm the presence of an extraterrestrial component in impactites and to determine the nature of the bolide. More detailed age dating is needed to provide a more precise age of the impact event than is known today. Furthermore, determination of shock levels in autochthonous rocks as a function of distance from the central uplift would be interesting.

Acknowledgments–The research was supported by Austrian FWF Projects P08794-GEO and Y58-GEO (to C. K.), and by a travel stipend of the University of Vienna (to E. G.). We are grateful to D. Brandt (University of the Witwatersrand, Johannesburg) for U-stage work and to D. Jalufka (Vienna) and D. du Toit and L. Whitfield (Johannesburg) for graphics. Detailed and helpful reviews by A. Deutsch, V. Masaitis, and A. Therriault led to a considerable improvement of this manuscript.

Editorial handling: A. Deutsch

REFERENCES

ANSHELES O. M. (1952) *The Beginnings of Crystallography* (in Russian). Leningrad University Press, Leningrad, Russia. 276 pp.

BISTREVSKAYA S. S., ZEMSKOVA G. A. AND VINOGRADOV G. G. (1974) New data of the Ilyinets paleovolcano structure on the Ukrainian Shield (in Russian). *Geol. J.* (Kiev) **34,** 123–126.

EMMONS R. C. (1943) *The Universal Stage (With Five Axes of Rotation).* Geological Society of America, Memoir 8. 205 pp.

ENGELHARDT W. V. AND BERTSCH W. (1969) Shock induced planar deformation structures in quartz from the Ries crater, Germany. *Contrib. Mineral. Petrol.* **20,** 203–234.

FELDMAN V. I. (1982) Some geochemical peculiarities of impactites (in Russian). In *Kosmicheskoe Vehestvo Na Zemle*, pp. 96–104. Naukova Dumka, Kiev, Ukraine.

GRIEVE R. A. F. (1978) The petrochemistry of the melt rocks at Brent crater and their implication for the condition of impact. *Meteoritics* **13,** 484–487.

GRIEVE R. A. F. AND ALEXOPOULOS J. (1988) Microscopic planar features in quartz from Scollard Canyon, Alberta, and the Cretaceous–Tertiary boundary event. *Can. J. Earth Sci.* **25,** 1530–1534.

GRIEVE R. A. F. AND ROBERTSON P. B. (1979) The terrestrial cratering record, I. Current status of observations. *Icarus* **38,** 212–229.

GRIEVE R. A. F., LANGENHORST F. AND STÖFFLER D. (1996) Shock metamorphism of quartz in nature and experiment: II. Significance in geoscience. *Meteorit. Planet. Sci.* **31,** 6–35.

GUROV E. P. AND GUROVA E. P. (1982) The peculiarities of shock metamorphism of volcanic rocks on example of the Elgygytgyn crater (in Russian). In *Geologia i Petrologia Vzrivnich Meteoritnich Kraterov* (ed. V.A. Ryabenko), pp. 83–89. Nauvova Dumka, Kiev, Ukraine.

GUROV E. P. AND GUROVA E. P. (1991a) On downward transport of matter at the impact crater formation (abstract). *Lunar Planet Sci.* **22,** 511–512.

GUROV E. P. AND GUROVA E. P. (1991b) *Geological Structure and Rock Composition of Impact Structures* (in Russian). Naukovka Dumka, Kiev, Ukraine. 160 pp.

GUROV E. P. AND RYABENKO V. A. (1984) Excursion 098: Impact structures of the Ukrainian Shield. In *27th International Geological Congress, Moscow, 1984*, pp. 143–159. Ukrainian Soviet Socialist Republic, Guidebook: Excursions 020, 023, 025, 081, 090, 095, and 098; Naukova Dumka, Kiev, Ukraine.

GUROV E. P. AND YAMNICHENKO A. Y. (1995) Morphology of rim of complex terrestrial craters (abstract). *Lunar Planet. Sci.* **26,** 533–534.

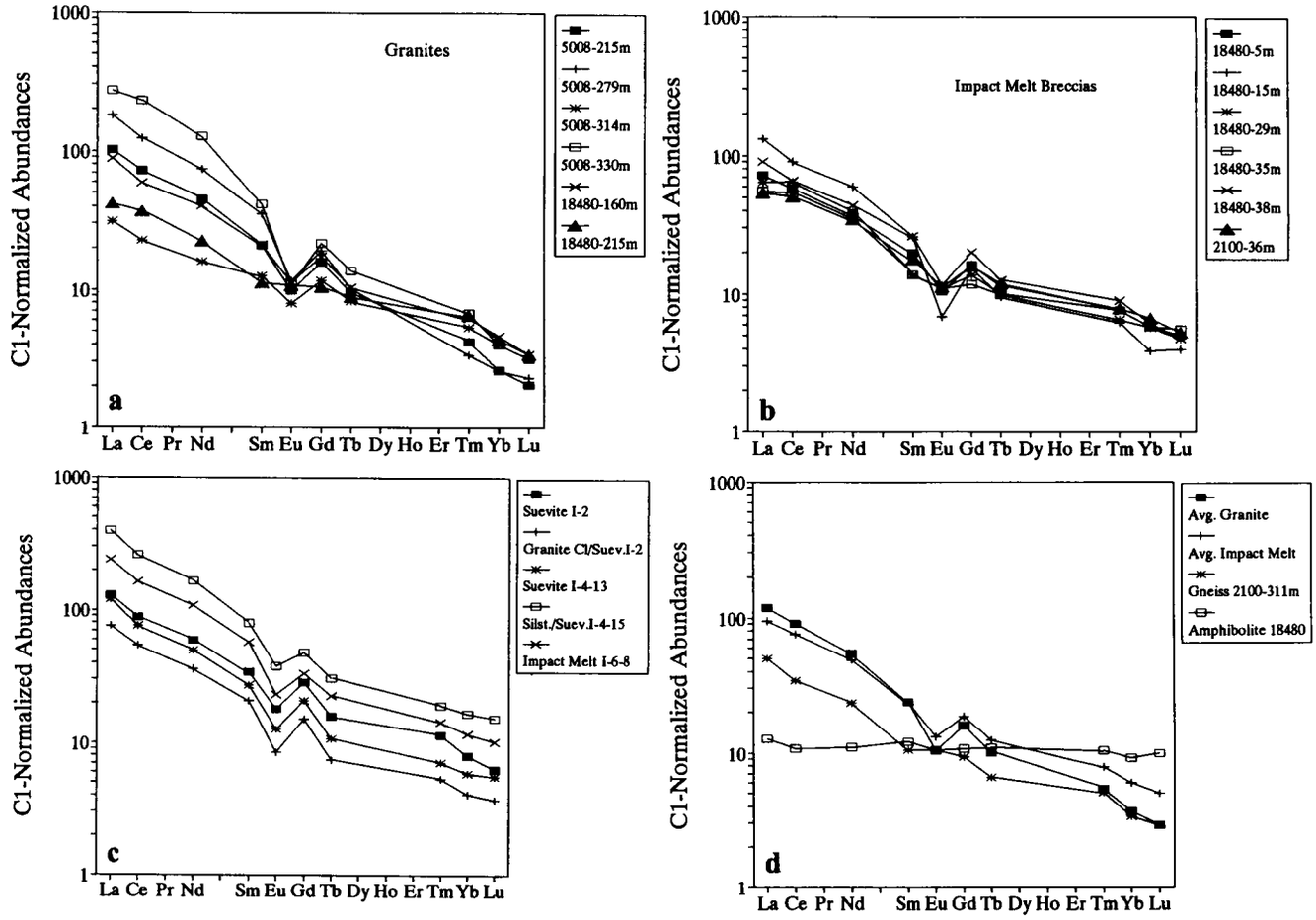

FIG. 10. Chondrite-normalized rare earth element (REE) abundance patterns for Ilyinets rocks; normalization factors from Taylor and McLennan (1985). Ranges of REE patterns (a) for granites, (b) for impact-melt rocks, (c) for suevites and clasts, and (d) for other rock types and average compositions.

GUROV E. P., GUROVA E. P. AND RAKITSKAYA R. B. (1979) Orientation of planar elements in quartz from the rocks of the meteorite impact craters (in Russian). *Zapisky Vseoyuzn. Mineralog. Obshestva* **5,** 578–584.

GUROV E. P., VALTER A. A. AND RAKITSKAYA R. B. (1980) Coesite in rocks of meteorite explosion craters on the Ukrainian Shield. *Int. Geol. Rev.* **22,** 329–332.

GUROV E. P., KOLESOV G. M. AND GUROVA E. P. (1986) Composition of impactites of the Boltysh astrobleme (in Russian). *Meteoritika* **45,** 150–155.

GUROV E. P., GUROVA E. P. AND RAKITSKAYA R. B. (1995a) Impact diamonds in the craters of the Ukrainian shield (abstract). *Meteoritics* **30,** 515–516.

GUROV E. P., GUROVA E. P. AND YAMNICHENKO A. Y. (1995b) The structure of complex impact craters and estimation of their preservation stage (abstract). *Lunar Planet. Sci.* **26,** 535–536.

GUROV E. P., GUROVA E. P. AND RAKITSKAYA R. B. (1996) Impact diamonds of the Zapadnaya crater: phase composition and some properties (abstract). *Meteorit. Planet. Sci.* **31 (Suppl.),** A56.

HÖRZ F. AND QUAIDE W. L. (1973) Debye–Scherrer investigation of experimentally shocked silicates. *The Moon* **6,** 45–82.

HUFFMAN A. R. AND REIMOLD W. U. (1996) Experimental constraints on shock-induced microstructures in naturally deformed silicates. *Tectonophysics* **256,** 165–217.

KINNUNEN K. A. AND LINDQVIST K. (1998) Agate as an indicator of impact structures: An example from Sääksjärvi, Finland. *Meteorit. Planet. Sci.* **33,** 7–12.

KOEBERL C. (1993) Instrumental neutron activation analysis of geochemical and cosmochemical samples: A fast and proven method for small sample analysis. *J. Radioanal. Nucl. Chem.* **168,** 47–60.

KOEBERL C., REIMOLD W. U. AND GUROV E. P. (1996) Petrology and geochemistry of target rocks, breccias, and impact melt rocks from the Ilyinets crater, Ukraine (abstract). *Lunar Planet. Sci.* **27,** 681–682.

KOEBERL C., MASAITIS V. L., SHAFRANOVSKY G. I., GILMOUR I., LANGENHORST F. AND SCHRAUDER M. (1997a) Diamonds from the Popigai impact structure, Russia. *Geology* **25,** 967–970.

KOEBERL C., REIMOLD W. U., BRANDT D., DALLMEYER R. D. AND POWELL R. A. (1997b) Target rocks and breccias from the Ames impact structure, Oklahoma: Petrology, mineralogy, geochemistry, and age. In *The Ames Structure and Similar Features* (eds. K. Johnson and J. Campbell), pp. 169–198. Oklahoma Geological Survey Circular **100,** Oklahoma, USA.

LANGENHORST F. (1993) Hochtemperatur–Stosswellenexperimente an Quarz–Einkristallen. Ph.D. dissertation, University of Münster, Germany. 126 pp.

LANGENHORST F. (1994) Shock experiments on pre-heated α- and β-quartz: II. X-ray and TEM investigations. *Earth Planet. Sci. Lett.* **128,** 683–698.

LANGENHORST F. AND DEUTSCH A. (1994) Shock experiments on pre-heated α- and β-quartz: I. Optical and density data. *Earth Planet. Sci. Lett.* **125,** 407–420.

MASAITIS V. L. (1973) *The Geological Consequences of Falls of Crater-Forming Meteorites* (in Russian). Nedra Press, Leningrad, Russia. 17 pp.

MASAITIS V. L., FUTERGENDLER S. I. AND GNEVUSHEV M. A. (1972) Diamonds in impactites of the Popigai meteorite crater (in Russian). *Proc. All-Union Mineral. Soc.* **1,** 108–112.

MASAITIS V. L., DANILIN A. N., MASCHAK M. S., RAYKHLIN A. I., SELIVANOVSKAYA T. V. AND SHADENKOV E. M. (1980) *Geology of Astroblemes* (in Russian). Nedra Press, Leningrad, Russia. 231 pp.

MELOSH H. J. (1989) *Impact cratering: A Geologic Process*. Oxford Univ. Press, New York, New York, USA. 245 pp.

NIKOLSKY A. P. (1975) The meteorite explosion craters of the Ukrainian Shield near Vinnitsa (in Russian). *Geol. J.* (Kiev) **35,** 76–86.

REIMOLD W. U. AND GIBSON R. L. (1996) Geology and evolution of the Vredefort impact structure, South Africa. *J. African Earth Sci.* **23,** 125–162.

REIMOLD W. U., KOEBERL C. AND BISHOP J. (1994) Roter Kamm impact crater, Namibia: Geochemistry of basement rocks and breccias. *Geochim. Cosmochim. Acta* **58,** 2,689–2,710.

REINHARD M. (1931) *Universaldrehtischmethoden*. Birkhäuser Verlag, Basel, Switzerland. 118 pp.

SOBOLEV V. S. (1954) *The Fedorov Method* (in Russian). Gosgeoltechnizdat, Moscow, Russia. 254 pp.

STÄHLE V. (1972) Impact glasses from the suevite of the Nördlinger Ries. *Earth Planet. Sci. Lett.* **17,** 275–293.

STÖFFLER D. (1972) Deformation and transformation of rock-forming minerals by natural and experimental shock processes: 1. Behaviour of minerals under shock compression. *Fortschr. Mineral.* **49,** 50–113.

STÖFFLER D. (1974) Deformation and transformation of rock-forming minerals by natural and experimental processes: 2. Physical properties of shocked minerals. *Fortschr. Mineral.* **51,** 256–289.

STÖFFLER D. AND GRIEVE R. A. F. (1994) Classification and nomenclature of impact metamorphic rocks: A proposal to the IUGS subcommission on the systematics of metamorphic rocks (abstract). *Lunar Planet. Sci.* **25,** 1,347–1,348.

STÖFFLER D. AND LANGENHORST F. (1994) Shock metamorphism of quartz in nature and experiment: I. Basic observations and theory. *Meteoritics* **29,** 155–181.

TAYLOR S. R. AND MCLENNAN S. M. (1985) *The Continental Crust: Its Composition and Evolution*. Blackwell Scientific Publications, Oxford, U.K. 312 pp.

VALTER A. A. (1975) Deciphering of the Ilyinets structure as astrobleme (in Russian). *Doklady Akademi Nauk SSSR* **224,** 1377–1379.

VALTER A. A. AND LAZARENKO E. E. (1982) The Ilyinets astrobleme (in Russian). In *Geologia i Petrologia Vzrivnich Meteoritnich Kraterov* (ed. V.A. Ryabenko), pp. 197–202. Nauvova Dumka, Kiev, Ukraine.

VALTER A. A. AND RYABENKO V. A. (1973) Petrological evidence of shock metamorphic origin of Ilyinets structure (in Russian). *Geol. J.* (Kiev) **33,** 142–144.

VALTER A. A. AND RYABENKO V. A. (1977) *The Impact Craters of the Ukrainian Shield* (in Russian). Naukova Dumka, Kiev, Ukraine. 156 pp.

YAKOVLEV O. I., PARFENOVA O. V. AND IGNATCHENKO K. I. (1982) Irregular condensation and ultra-potassium impactites (in Russian). *Meteoritika* **41,** 141–149.